Anderson Hanna (Orcid ID: 0000-0002-1497-3650)

Accelerated sediment phosphorus release in Lake Erie's central basin during seasonal anoxia

Hanna S. Anderson[1*], Thomas H. Johengen[1], Russ Miller[1,] and Casey M. Godwin[1]

*Corresponding author: Hanna S. Anderson, hannaand@umich.edu

[1]Cooperative Institute for Great Lakes Research (CIGLR), School for Environment and Sustainability, University of Michigan, Ann Arbor, MI, USA

Author email addresses: Hanna S. Anderson, hannaand@umich.edu; Thomas H. Johengen, johengen@umich.edu; Russ Miller, rusmil@umich.edu; Casey M. Godwin, cgodwin@umich.edu

Key words: Lake Erie, internal phosphorus loading, phosphorus sediment flux, anoxia, eutrophication

Author Manuscript

This is the author manuscript accepted for publication and has undergone full peer review but has not been through the copyediting, typesetting, pagination and proofreading process, which may lead to differences between this version and the Version of Record. Please cite this article as doi: 10.1002/lno.11900

This article is protected by copyright. All rights reserved.

Author Manuscript

Abstract

Eutrophication remains a serious threat to Lake Erie and has accelerated over past decades due to human activity in the watershed. Internal phosphorus (P) loading from lake sediment contributes to eutrophication, but our understanding of this process in Lake Erie is more uncertain than for its riverine P inputs. Past work has focused on incubating sediment cores in oxic or anoxic conditions, meaning we know little about sediment flux during state transitions. We used fifty-six controlled sediment core incubation experiments to quantify rates and onset of P release in Lake Erie's central basin as a function of depositional environment, season (spring, summer, and fall), temperature, and dissolved oxygen (DO) concentration. P flux under oxic or hypoxic (>0 to ≤2 mg L^{-1} DO) conditions was slow (0.31 – 0.50 mg m^{-2} day^{-1}) compared to anoxic P flux (5.19 – 30.7 mg m^{-2} day^{-1}). The transition between slow and fast flux occurred within 24 hours of anoxia (0 mg L^{-1} DO). Oxic or anoxic P flux was generally similar across seasons and incubation temperatures (8 and 14ºC). In 14°C incubated cores anoxic P flux onset was earliest in fall, when sediments had already been exposed to anoxic conditions in the lake. Re-oxygenation of experimental cores that temporarily developed anoxia reversed the direction of P flux, but P release resumed at similar rates once the water returned to anoxia. Understanding the effects of hypolimnion oxygen conditions on internal P loading allows us to better constrain nutrients sources and implications for P budget management.

Author Manuscript

Introduction

Lake Erie has a history of environmental degradation, and past industrial and wastewater runoff led to eutrophication throughout the lake (DePinto et al., 1981). Consequences of eutrophication have included promotion of harmful algal blooms (HABs) in the western basin and summertime hypoxia in the central basin. Environmental regulations such as the U.S. Clean Water Act (CWA, 1972) forced the management of point source pollution, and many of the ecological consequences of pollution were diminished or abated for a time (Scavia et al., 2014). Despite recent management efforts targeting point source nutrient pollution from Lake Erie's watershed, both HABs and hypoxia remain problems for the lake (Scavia et al., 2014), in part due to continued land use changes and agricultural practices. In Lake Erie and other aquatic environments, hypoxia changes food web structures, biogeochemical cycling in the water and sediment, habitat availability, and life cycles of key species (Stone et al., 2020; Foster and Fulweiler, 2019). The spatial extent of hypoxia and anoxia (0 mg L^{-1} DO) in Lake Erie within a given year is dependent on thermal structure and the timing of stratification (Beletsky et al., 2013), hydrodynamic movements (Rowe et al., 2019), and wind stress. Over longer timescales, studies have shown that hypoxia in the central basin is related to, and has recently expanded in response to, increased tributary P discharge (Zhou et al., 2013; Edwards et al., 2005). Nutrient loading reductions are prioritized as a means to minimize hypoxia and other symptoms of eutrophication, and although interannual variability in P loading is well understood in the western basin (Matisoff et al., 2016; Scavia et al., 2017b; Rowland, et al., 2020), improved characterization of P loading and sources is needed for the central basin (Mohamed, 2019).

Another input of nutrients comes from the recycling of legacy P inputs stored in lake sediments via internal phosphorus loading, a potentially important component of a lake's P

Author Manuscript

budget (Nürnberg, 1984; Nürnberg, 1991). A major driver of internal P loading occurs when low dissolved oxygen (DO) conditions and redox conditions at the sediment-water interface allow for inorganic P to flux out of the sediment (Foster and Fulweiler, 2019). Eutrophication can exacerbate internal loading as excess growth of algal biomass can later fuel increased oxygen consumption in the hypolimnion. Decaying organic matter from algal blooms is remineralized as it integrates into lake sediment, creating a reservoir of nutrients over time (Gerling et al., 2016) and driving respiration of dissolved oxygen (Reavie et al., 2016). Under oxic conditions, iron oxides (such as Fe III oxyhydroxides) are powerful sorbents of inorganic phosphorus (Davidson, 1993) but when DO is absent, microbes respire these oxides and convert them to a soluble form that releases bound inorganic P (Boström et al., 1998; Mortimer, 1971). This results in internal phosphorus flux as inorganic P diffuses into the water (Steinman and Spears, 2020). This effect, known as "accelerated eutrophication", has been suggested for various water bodies (Caraco, 2009; Vahtera et al., 2007) and can act as a positive feedback mechanism that complicates efforts to control eutrophication through limiting loading from the watershed (Steinman and Spears, 2020). Although this mechanism is well recognized, there is uncertainty as to the relationship between watershed loading of P and hypoxic extent in the central basin of Lake Erie (Scavia et al., 2017a).

The morphological and physical conditions of Lake Erie's central basin make it especially susceptible to widespread anoxia and internal phosphorus loading compared to other large lakes. In the central basin (max depth 25 m) seasonal thermal stratification and basin morphology yield a warm, thin hypolimnion often only 2-3 meters thick. Organic matter production in the basin creates high oxygen demand and adds a large supply of nutrients to the surface sediment, leading to recurring seasonal hypoxia and anoxia. Lake Erie has specific areas

Author Manuscript

that are spatially and temporally vulnerable to hypoxia and anoxia, including the Ohio shoreline of the central basin (Rowe et al., 2019). Lake Erie's large-scale occurrence of low DO conditions and internal loading makes it an important system in which to study these processes.

There are a few recent experimental measurements of internal P loading for the central basin, but available estimates show highly divergent rates. Matisoff et al. (1977) performed a sediment core incubation study and found anoxic P flux from 12.8 to 73.5 mg m^{-2} day^{-1} at 14-16°C. More recently, Paytan et al. (2017) incubated central basin sediment cores at 7°C and calculated anoxic P flux as 0.32 mg m^{-2} day^{-1} and oxic P flux at 0.58 mg m^{-2} day^{-1}. Paytan's incubation experiment occurred after cores were stored for a 2-month period which, combined with a relatively low incubation temperature, may explain the difference in this anoxic P flux estimate relative to others. Nürnberg et al. (2019) presented a different approach that combined summer water collection data showing TP increases over 9 years, in situ hypolimnion P concentration change data from Burns and Ross (1972), and total surface sediment P concentrations from an earlier study (Nürnberg, 1988), which estimated hypoxic P flux at 7.6-8 mg m^{-2} day^{-1}.

In addition to the limited number of measurements of P flux from Lake Erie, there is also a lack of consensus regarding the conditions that result in accelerated P flux. Some models assume that accelerated flux begins at varying definitions of anoxia, some at 1.0 mg DO L^{-1} and others at 1.5 mg DO L^{-1} (Zhang et al., 2016). Since estimates of internal loading are critically dependent on the area and duration of sediments that are undergoing accelerated P flux, we need to understand precisely the DO conditions that lead to flux. Pinpointing these conditions is especially important in Lake Erie, where hypoxia and anoxia exhibit dramatic inter-annual variability (Zhou et al., 2013), and advection or upwelling can disrupt stratification and

Author Manuscript

hypolimnion anoxia, causing abrupt changes in the redox condition at the sediment-water interface (Ruberg et al., 2008). Detailed continuous monitoring in Green Bay, Lake Michigan by Zorn et al. (2018) showed that turnover events and subsequent re-stratification had mixed effects on hypolimnion phosphorus concentration and DO consumption during organic matter remineralization, but the effects on P flux were not fully characterized. Our study mimics re-stratification events in experimental cores in order to observe and replicate the conditions and rates of P release in response to short-term disruptions of the hypolimnion at a fine scale. To complement this incubated sediment core study, we also performed continuous in situ monitoring in Lake Erie's central basin where we monitored a hypolimnion disruption event and observed that average P flux was higher after this disturbance than before (Anderson et al., 2021).

Our study used a series of controlled sediment core incubations to quantify: 1) oxygen conditions required for the onset of P flux, 2) rates and timing of phosphorus flux with respect to location in Lake Erie's central basin, temperature, time of year, and DO conditions, and 3) behavior of P flux following a hypolimnion-disturbing event.

Materials and methods

We sampled sediment cores at three locations in Lake Erie's central basin in order to represent differing depositional environments (Figure 1). These locations were each adjacent to instrumented moorings that continuously recorded temperature and dissolved oxygen throughout the water column. Sediment coring at site CB5 took place several kilometers offshore from the site due to non-depositional and uncoreable substrate at the mooring location. Detailed descriptions of the locations and environmental context of the moorings are available in the NOAA National Centers for Environmental Informatics (NCEI, www.ncei.noaa.gov) under

Accession numbers 0210815, 0210823; and 0210822. Coring experiments were performed during spring (June 4-5), summer (July 24-25), and fall (September 18-19) of 2019.

Figure 1: Map of Lake Erie including the three central basin (CB) coring sites. The three depth contour lines represent water column depths of 10, 15, and 20m.

Each season, cores were collected over a span of 2 days, with all cores from a single site collected at the same time. An Ekman box corer (30 x 30 cm) was used to retrieve large, undisturbed sediment samples (>0.5 m thickness) and overlying hypolimnion water from each site. Experimental cores were manually collected from the box core using polycarbonate cores with a total length of 30.5 cm and diameter of 14.6 cm. Only one experimental core was extracted from each box core due to disturbance of the sediment surface during collection. Each core contained an average of 2,130 cubic cm of sediment and 1,723 mL of overlying hypolimnion water. The experimental cores were based on the design of Arega and Lee (2005) and were sealed at the top with an air-tight core lid (details below) and an expanding plug below the sediments. In addition to the experimental cores, a small 3 cm diameter core was collected from each box core, from which we extruded and froze the top 1 cm for elemental analyses (methods and results available in Supplemental Information).

During each sampling event, 100 L of hypolimnion water was collected using a submersible pump coupled to a water quality sonde (YSI EXO2 Multiparameter Sonde) to monitor collection conditions. This water was used as overlying water during sediment core incubations. A small sample of this overlying water was filtered and analyzed for soluble reactive phosphorus (SRP) concentration as described below. The lake was not strongly stratified for the June collection, so water was collected 4-5 m from the bottom. At each sampling site, care was taken to avoid collecting water from areas where the hypolimnion was disturbed by

Author Manuscript

sediment coring. Table 1 lists ambient lake water temperature, dissolved oxygen, conductivity, and pH at the time of each sampling. Exact sediment coring depths varied between seasons due to lake bathymetry, but were approximately 21.5 m at CB2, 24.5 m at CB4, and 22 m at CB5. After collection, experimental sediment cores and water samples were transported to the Great Lakes Environmental Research Laboratory (GLERL) in Ann Arbor, MI. The cores remained sealed, shielded from light, and cooled with ice for the average 8 hours of transport time from collection to laboratory.

Author Manuscript

Author Manuscript

Table 1: Summary of 2019 coring dates and locations with accompanying sonde data.

		Date Cored	Water Sampling Depth (m)	Bottom Temp (°C)	Bottom Dissolved Oxygen (mg L^{-1})	Hypolimnion SRP (µg L^{-1})	Conductivity (µS cm^{-1})	pH
Spring	**CB2**	**June 4**	15.0	12.5	10.3	0.96	255	7.98
	CB4	**June 5**	20.5	8.10	9.50	2.11	268	7.67
	CB5	**June 5**	21.6	8.30	9.80	2.32	267	7.71
Summer	**CB2**	**July 25**	20.8	12.4	5.40	2.92	284	7.50
	CB4	**July 24**	23.6	8.50	6.34	3.32	279	7.45
	CB5	**July 24**	22.8	10.4	6.56	4.54	277	7.57
Fall	**CB2**	**Sep. 19**	16.6	12.3	0.07	36.6	279	7.71
	CB4	**Sep. 18**	23.8	11.0	0.02	34.2	283	7.08
	CB5	**Sep. 18**	21.1	12.0	0.02	28.1	278	7.33

Sediment core chambers were designed as closed circulation systems (Figure 2) (Arega and Lee, 2005). The design and hydraulics of this core incubation setup were shown to be useful for observing exchange processes across the sediment-water interface (Arega and Lee, 2005; Lee et al., 2000). Core chambers had one central output and two input jets for water circulation, all located at the top of the core. The circulation systems consisted of 3.12 mm tubing (Cole-Parmer EW-06440-16) connecting the sediment core, a reservoir, and a dissolved oxygen sensor (PME MiniDOT) with flow-through adapter to a peristaltic pump (see Figure 2). Airtight compression fittings were used to connect the tubing to the incubated cores to prevent gas exchange. Sampling ports associated with each core allowed us to sample overlying water throughout the incubation period, and input and withdrawal ports were physically separated within the flow system to prevent short-circuit uptake in the withdrawn sample. In order to prevent readings in stagnant

Author Manuscript

water, which is problematic for optical DO sensors, we built flow cells to ensure the DO sensors were exposed to high-velocity water in the circulation system. One potential shortcoming of this experimental setup is that the reservoirs and circulation system may create micro-environments that are slightly different from the overlying water in the core. While the water circulation ensured that these volumes were well-mixed, small differences in the oxygen concentration between the sensor sediment surface may slightly impact our estimates of the dissolved oxygen concentration at which accelerated P flux begins.

On each date (Table 1) we collected 6 cores from each sampling station. We randomly divided the cores from each site into triplicates incubated at 8ºC and triplicates incubated at 14ºC. Among the three stations, this yielded a total of 9 cores incubated at 8ºC and 9 cores incubated at 14ºC during each season. Cores from each season were incubated at both temperatures in order to control for seasonality and temperature variables, although not every temperature and season combination represents realistic in situ conditions. In particular, the temperature of the hypolimnion in summer (July) is likely more variable than the other seasons and depends on location within the basin and water circulation (Rowe et al., 2019). All 9 cores at each temperature were incubated in a common, darkened environmental chamber. Each core had a separate reservoir, DO sensor, and tubing. Flow was maintained by multichannel peristaltic pumps, each of which controlled 3 or 4 cores.

Figure 2: Diagram of the core incubation system used for the experiments. Components include sediment core chamber, peristaltic pump, overlying water reservoir, dissolved oxygen sensor, and connective tubing with sampling ports. Arrows indicate direction of water flow.

Upon return to the laboratory, cores were placed within the incubators and allowed to settle for 30 minutes. Each incubator contained 9 cores, three from each coring site. Stainless

steel jets that allowed circulating water to enter the sediment core chamber were adjusted so that the outlets were fixed approximately 3-4 cm above the sediment pointing in opposite directions to create well-mixed conditions with velocities of ~1-3 cm s^{-1} that approximated the predominantly horizontal water velocities expected near the sediment surface without disturbing the sediment and causing release of P due to high water velocity (Lee et al., 2000; Arega and Lee, 2005; Ivey and Boyce, 1982). After settling, the cores were flushed with unfiltered site water (containing all the biota naturally present in the hypolimnion) sampled at the time of coring to replace the original water from the system and minimize the effects of any disturbed sediment from transport in order to start with fully oxygenated conditions. After the flushing process, we began a period of open circulation during which the unfiltered overlying water was re-circulated through an open bath inside the incubator. This open circulation was intended to ensure that overlying water was saturated with DO prior to sampling. The peristaltic pumps operated at 125 mL min^{-1} during the 60-minute flushing process and the 8-hour open exchange.

Closed circulation began when the reservoir output tube was attached to the input of the DO sensor and the sensor was removed from the bath. Each sediment core incubation system was checked for air bubbles. To displace any headspace remaining in the components, replacement overlying water was added via the input port. Circulation rates during the experiment were set based on the chamber design paper (Arega and Lee, 2005) to mimic published accounts of lake bottom conditions (Snodgrass et al., 1987) with the goal of not disturbing the sediment-water interface. During the first 24 hours of closed circulation when DO was > 4 mg L^{-1}, peristaltic pump speeds were varied every few hours between 50, 125, and 250 mL min^{-1} as an experimental variable to examine flow rate effect on sediment oxygen demand rates (Arega and Lee, 2005). Following this period, and when DO was still > 3 mg L^{-1}, pump

Author Manuscript

Author Manuscript

speeds were maintained at a fixed rate of 125 mL min^{-1} for the remainder of the experiment including the transition to anoxia.

During incubation, dissolved oxygen and temperature were recorded every 60 seconds and water samples for SRP concentration were taken at discrete time points (6-24 hour intervals) over the course of the incubation in order to capture P flux behavior across the range of DO conditions. We assumed steady-state DO condition throughout the system. Although it is possible that the sediments reached anoxia before the overlying water was completely anoxic, we aimed to quantify the onset with respect to dissolved oxygen in the water, which is more readily and frequently monitored than sediment conditions. Core water samples were collected using syringes via the sampling port system at least once every 24 hours while DO consumption rates were low, and more frequently when core water approached hypoxic conditions (2 mg L^{-1} DO). To collect each sample, 45 mL of water was removed through one port while an equal amount of temperature-equilibrated overlying water was added back via the second port with another syringe. Water samples were immediately filtered into test tubes from collection syringes using membrane filters with a 0.2 µm pore size and frozen at -20ºC until analysis. Total incubation length ranged from 12-16 days, with variation between seasons based on the amount of time needed for complete depletion of dissolved oxygen.

Following at least 4 days of sustained anoxia, a subset of cores incubated at 14ºC were re-aerated in order to observe how sediment P flux responded to conditions of short-term replacement of local anoxic water with normoxic water. We did not perform replacements for the 8ºC cores as they generally took much longer to reach anoxia, and such long incubation times eventually decreased the efficacy of the incubation systems. The purpose of re-aeration was to mimic replacements of hypolimnetic water, which have been observed in Lake Erie (Ruberg et

Author Manuscript

al., 2008). This re-aeration experiment was repeated in the spring, summer, and fall and involved replacing the overlying incubation water from selected core replicates with oxygenated hypolimnion water collected from each site. The average SRP concentrations from the 14°C re-aerated core overlying water before and after re-aeration were 232.1 µg L^{-1} and 43.3 µg L^{-1}. This means that while the volume of the cores remained the same, the sediment-water concentration gradient dropped so that flux would not be gradient-limited following re-aeration. This water replacement was slow enough as to not disturb the sediment and expose a new surface to the new overlying water. The re-aeration experiment was performed in 2 of the 3 cores from each sampling location while the third core was left undisturbed. This re-aeration experiment mimics sudden replacements of overlying water with some caveats. The sediment cores are volume-limited, meaning SRP accumulates in the fixed overlying water volume, causing the sediment-water concentration gradient to become more severe. This limits P release from surface sediments after prolonged incubation relative to the natural system. Additionally, the re-aeration experiment does not re-establish the depth of oxic penetration in the sediment that was present before coring, so the second P flux may happen earlier than in an in situ re-aeration scenario with longer re-exposure to oxic conditions. These nuances are reflective of the variations of in situ hydrodynamic movements that lead to anoxic water being rapidly replaced with oxic water.

Samples from both the sediment cores and the original overlying water were analyzed for soluble reactive phosphorus (SRP) using a Seal AA3 auto-analyzer using the molybdate blue reaction (Method No. G-297-03 Rev. 5 Multitest MT 19). SRP standards were prepared daily from a NIST-traceable stock (Hach Company). Preliminary experiments revealed that anoxic water could cause matrix effects with this analytical method, possibly due to co-elution of dissolved iron from sediments, so samples were diluted with deionized water at a range of

concentrations. All samples were run in duplicate and the median relative standard deviation among replicates was 2.01%. The analytical detection limit was 1 µg L^{-1}, and diluted samples had proportionally higher detection limits. Several samples were below detection limits, and these were primarily immediately following re-aeration and were omitted from the regressions. This study focuses on release of soluble reactive P and therefore all reported P flux estimates refer to phosphorus in the form of SRP.

P flux from sediment to water was calculated using the change in concentration of SRP in water over time. We estimated this rate in two or three different phases in each core, shown in Figure 3. Similar to previous work (Anderson et al., 2021), we did not find accelerated increases in SRP until close to or after the onset of anoxia. To account for the dilution or addition of P due to each sampling and water replacement (on average 1.2% of the total overlying volume), we estimated the cumulative total P released from the sediment at each timestep using Equation 1.

Equation 1: $m_t = m_{t-1} + v_{total}(c_t - (c_{t-1} \times \frac{V_{total} - V_{removed}}{V_{total}} + c_{OLW} \times \frac{V_{removed}}{V_{total}}))$

In Equation 1, m_t and m_{t-1} are accumulated masses of P in the water (mg P per core), c_t is the concentration at time t, c_{t-1} is the concentration measured at the previous time point, c_{OLW} is the concentration of P in the overlying water that was added when a sample was removed, V_{total} is the total water volume in the incubation system, and $V_{removed}$ is the volume of water removed from the system at each sampling time point. We performed this adjustment calculation for each timestep except for the re-aeration events, where we used the first measurement following water replacement for the first timepoint.

The P accumulation data was used to calculate P release rates from the sediment during normoxic and anoxic conditions. We set the timescale for each core to begin (t = 0) at the onset of anoxia based on each core's DO data. This allowed us to express the timing of flux

Author Manuscript

Author Manuscript

acceleration with respect to the onset of anoxia without affecting the rates found during oxic or anoxic conditions. In order to estimate both rates and the transition time at which the flux accelerates (the onset timing), we fitted segmented linear regressions to accumulated P versus time elapsed. Throughout this paper, this accelerated flux under anoxia is termed anoxic P flux. Only anoxic P rates were calculated during re-aeration as rapid DO consumption under these conditions made it difficult to fit reliable oxic P rates.

Onset of anoxic P flux was calculated relative to the time when each core first experienced anoxic conditions. Conventional definitions of anoxia as a nominal zero DO concentration and noted experimentally by minimum DO readings for each sensor (with a range of 0.007-0.020 mg L^{-1}), were used as the indication for anoxia onset during incubation. This lower limit was determined by incubating all sensors in water dosed with potassium meta-bisulfite where anoxia was confirmed with Winkler titrations. Anoxic P flux onset (hours) was calculated as the difference between the time of the last dissolved oxygen measurement above anoxia and the transition time to anoxic P flux in each incubating core. While sampling was done at regular intervals during the transition to anoxia, in some cases lower sampling frequency led to increased uncertainties in the estimations of transition time to anoxic P flux. Sampling frequency was increased during the re-aeration experiment in order to capture faster expected P flux, and although this increased accuracy for this part of the experiment, it introduced a possible source of error in terms of sampling rate bias relative to the initial portion of the experiment.

In order to derive estimates of rates and timing from all of the available data, we fit the segmented regressions using a hierarchical Bayesian framework. This approach is similar to a mixed-effects regression model, with fixed effects and random effects for each replicate, but has the advantage of using all the information to help constrain estimates at the innermost level (e.g.,

Author Manuscript

individual cores or replicates from the same season and station) without requiring interaction terms. All analyses were performed in R (Version 4.0.2) using the package "brms" (Bürkner, 2018) to compile Bayesian regression models that were fitted using a Hamiltonian Markov Chain Monte Carlo algorithm in "stan" (Stan Development Team, 2020). Anoxic P flux calculations were constrained to the four days immediately following anoxia to avoid incorporating slower rates and other artifacts that occur after extended periods of anoxia in the volume-limited sediment cores. We made separate models for cores incubated at 8°C, cores incubated at 14°C prior to the re-aeration experiment, and cores incubated at 14°C during the re-aeration experiment. Within each hierarchical regression the outermost grouping term was season followed by station and core. Both the slopes and intercepts were allowed to vary among each level of the hierarchy.

We calculated the mean, standard errors, and credible intervals (95%) for each model parameter using the posterior distribution. Estimates from the posterior distribution represent the deviation from the overall mean rate. Each regression was informed by four Markov chains and weakly informative priors for the oxic P flux (location = 0, standard deviation =10), the transition time (10, 5) and the anoxic P flux (0, 10). After 1000 warmup iterations, each chain was sampled for 1000 iterations. We assessed that the cores had converged using the Gelman-Rubin statistic, which was $\hat{R} < 1.01$ in all cases (Gelman et al., Ch. 11, 2013).

Select contrasts between stations, seasons, experimental period, and temperatures were tested using the function "hypothesis" to examine support for select post-hoc contrasts. A sample hypothesis that would prove an evidence ratio might be, "Anoxic P flux is greater than oxic P flux". To test this hypothesis, we chose to use evidence ratios (ERs), or the ratio of the number of posterior samples consistent with the hypothesis to the number of posterior samples that are

Author Manuscript

inconsistent with the hypothesis, to assess strength of support for each contrast. While we did not assign an arbitrary cutoff value to these ERs, we interpret contrasts with low ER (<5) as having low or no support (Gelman et al., Ch. 5, 2013). We compared fluxes among different models by tabulating the differences between posterior draws and calculating mean differences and ERs as described previously. One core replicate from spring CB2 at 14°C was lost due to incubation system failure, so data from this core are not presented. Several cores incubated at 8°C (including all cores from spring CB4) never reached anoxia due to the temperature limitations on oxygen consumption and higher initial DO solubility, so although samples were analyzed, no fluxes or lag times were calculated.

Results and discussion

During the first portion of the experiment, SRP concentration was uniformly low until anoxia onset, when it began increasing due to flux from the sediment (Fig. 3). During the re-aeration experiment, SRP concentration dropped when the overlying water was removed and replaced with oxygenated (and low-P) water. After the water exchange, SRP concentrations continued to decrease until DO was completely depleted and anoxic P flux from the sediment resumed.

Figure 3: Dissolved oxygen and soluble reactive phosphorus (SRP) concentration over time for spring 2019 core M from site CB2. The blue vertical line represents the onset of anoxic P release during the first portion of the experiment and the black vertical line denotes the beginning of the re-aeration experiment. Labeled flux regions denote time periods where the shown SRP concentrations will be used to calculate fluxes.

Onset of anoxic P flux

Author Manuscript

Table 2 shows that spring and summer sampled cores incubated at 14°C had longer mean lag times (8.66 and 8.90 hours respectively) than fall cores, which displayed a negative mean lag time of -1.26 hours across all sites (i.e., accelerated flux began before anoxia). Lag timing in Table 2 refers to the time between anoxia onset and the time of anoxic P flux onset.

These results show clearly that the accelerated P flux we observed is a symptom of anoxia and not hypoxia, with the notable exception of anoxic P flux occurring hours prior to anoxia in fall. This trend in fall suggests that once sediments have experienced low-DO conditions in situ, as was true for the fall-sampled sediments (Table 1), accelerated soluble P release can occur prior to or upon anoxia onset. This response difference is likely due to a build-up of reduced substances and P in porewater just below the sediment-water interface such that diffusion within the sediment had stronger influence in advance of redox driven release. These reduced substances build up when there is no dissolved oxygen, a normally abundant electron acceptor, to respire them. Metal oxide reduction (including Fe) has been shown to begin prior to anoxia, mobilizing bound P across the sediment-water interface multiple times before full release into overlying water (Hupfer and Lewandowski, 2008; Foster and Fulweiler, 2019).

Author Manuscript

Table 2: Mean estimates of timing (hours with standard error), representing the difference between anoxia onset and anoxic P flux onset for 2019 sediment cores by temperature, season, and central basin (CB) sampling site.

		Hours Between Anoxia and Anoxic P Flux Onset	
		Cores Incubated at 14°C	**Cores Incubated at 8°C**
Spring	**All**	8.66±11.9	20.4±12.5
	CB2	18.0±17.3	17.5±11.3
	CB4	5.57±9.60	NA
	CB5	7.18±11.3	20.2±12.1
Summer	**All**	8.90±11.1	28.0±13.7
	CB2	5.49±9.54	23.5±12.1
	CB4	-1.01±10.4	33.9±19.8
	CB5	27.4±15.5	30.6±17.5
Fall	**All**	-1.26±11.5	23.6±10.2
	CB2	-2.59±10.3	27.1±12.3
	CB4	-3.39±9.34	22.8±8.96
	CB5	-6.48±10.7	19.8±9.36

Oxic and anoxic P flux

Table 3 shows that oxic P flux was lower than anoxic P rates across all seasons, stations, and temperatures. Rates within each phase of the experiment were similar across stations, seasons, and temperatures with some evidence of trends within these categories.

In 14°C cores, anoxic P flux prior to re-aeration ranged from 5.19 – 30.7 mg m^{-2} day^{-1} with an overall mean of 12.8 mg m^{-2} day^{-1} across all seasons and stations. Oxic P flux for 14°C incubated cores ranged from 0.31 – 0.50 mg m^{-2} day^{-1} with an overall mean of 0.38 mg m^{-2} day^{-1}.

Author Manuscript

There was no evidence for differences in oxic P flux between seasons when considered across or within stations. 14°C anoxic P flux was also similar across seasons. However, there was evidence that fall rates were lower than other seasons within stations. This may be due to a higher SRP concentration in the hypolimnion (28.1-36.6 μg L^{-1} in fall versus 2.92-4.54 μg L^{-1} in summer), which could decrease the concentration gradient at the sediment surface and decrease P flux as a result. These hypolimnion sample concentrations were taken at the time of coring and were 6-38x higher during fall across all sites than during spring and summer. Additionally, fall cores had previously experienced low-DO conditions, meaning a portion of the sediment metal oxides may have already been respired and released bound P. This previous P release would mean that fall sediments had a smaller source of bound P relative to other seasons, depressing P flux levels.

As expected, mean anoxic P flux was higher than mean oxic P flux in cores across both temperatures by a factor of 34-55 times. This finding matches the previous results of Matisoff et al. (2016) whose sediment cores from the Western Basin of Lake Erie showed that anoxic P flux was 4-13 times higher than oxic P flux. In terms of previous central basin estimates, anoxic flux reported here are within the range of anoxic P flux (12.8-73.5 mg m^{-2} day^{-1}) from Matisoff et al.'s 1977 sediment core incubations, but higher than those reported by Nürnberg et al., 2019 (7.6 – 8.0 mg m^{-2} day^{-1}). These differences are likely due to the methodology of the different approaches (i.e., core incubations versus estimating flux from changes in in situ SRP concentration). In our parallel in situ mooring study, average anoxic P flux before re-aeration was 11.42 ± 2.6 mg m^{-2} day^{-1} (Anderson et al., 2021). Our mean estimates are generally higher than previous estimates from the central basin, but our range of release rates is inclusive of sediment coring experiment estimates from other lakes such as Matisoff et al.'s 2016 western

basin rates of 6.56 ± 6.05 mg m^{-2} day^{-1}, James (2012) who reported anoxic P flux of 8.3-12.5 mg m^{-2} day^{-1} for Lake of the Woods, Minnesota, and Debroux et al. (2012) who estimated anoxic P flux of 6-8 mg m^{-2} day^{-1} from Lake Bard, California. Additionally, Lake Erie central basin P release rates are representative of other eutrophic lakes, (Phillips et al., 2020; Nürnberg, 1997).

Our findings signal that there is a period of time after hypoxia and before anoxia when phosphorus flux is occurring at rates several times slower than anoxic P release rates, and also a lag between anoxic onset and anoxic P flux onset. This timing can be affected if there is a sediment history of anoxic exposure, where previous exposure shortens the time before anoxic P flux onset. Results from this study show that regardless of whether sediments have previously experienced anoxia or are under unfavorable temperature conditions for DO consumption, magnitude of anoxic P flux is similar once accelerated flux begins. Finally, this study measured DO conditions of overlying water rather than of sediment pore water or sediment redox potential. While this approach does not reflect conditions in the sediment, it does relate the flux and onset to dissolved oxygen in the overlying water, which is more readily monitored and makes the results relatable to both modeled and measured patterns of oxygen in the basin. Therefore, we are reporting on the necessity of anoxic conditions in the overlying water to produce this accelerated flux.

Re-aeration experiment anoxic flux

Table 3 shows that re-aerated anoxic flux was similar across stations and seasons with some trends within stations. For re-aerated 14°C cores, anoxic P flux after re-aeration ranged from 5.08 – 61.0 mg m^{-2} day^{-1}, with a mean of 14.8 mg m^{-2} day^{-1}. We found no evidence that re-aerated anoxic P flux differed between seasons across all stations, however there was strong evidence that summer CB4 rates were higher than fall or spring (ER = 166 and 168,

Author Manuscript

Author Manuscript

respectively). When comparing between anoxic P flux and re-aerated anoxic P flux at 14°C, there was no difference at the level of season. The only strong evidence found was that re-aerated anoxic P flux was higher than initial anoxic P flux at CB4 in both spring and summer (ER = 7.21; 799) (see Fig. 4). Anoxic P flux did not change pre- and post-re-aeration, suggesting that re-aerated anoxic P flux behaves similarly in magnitude to the initial anoxic P release rates despite observed faster consumption of DO following re-aeration (seen in Figure 2). It is likely that a build-up of reduced substances at the sediment-water interface and in the overlying water following anoxia contributed to accelerated DO consumption.

There are previously reported rates and trends published for re-aerated sediment P release. Zorn et al. (2018) reports average release rates of 20.74 ± 23.3 mg m^{-2} day^{-1} following 8 re-aeration events observed in Green Bay using in situ instrumentation. There was no distinct trend in the 8 reported release rates relative to each other, attributed to different sets of properties driving water replacement and P release. Anderson et al. (2021) deployed in situ DO and SRP sensors at the CB2 and CB4 stations used in the present study and found that rates before re-aeration (11.42 ± 2.6 mg m^{-2} day^{-1}) were lower than re-aerated rates (89.1 ± 8.6 mg m^{-2} day^{-1}). There are several potential reasons why the re-aerated rates in the present study were not as high as those observed in Anderson et al. (2021). This in situ study was subject to advection of water during anoxia, which may have increased SRP concentration faster than from sediment flux alone. Also, the sediment core incubation had a lower ratio of overlying water to sediment, which could result in faster buildup of SRP in the water, thereby lowering the release rate from sediment.

Temperature effects

Author Manuscript

Comparisons between incubation temperatures showed compelling results in flux onset timing and oxic P flux magnitudes. The overall mean time difference from anoxia to anoxic P flux onset for cores incubated at 8°C was 23.4 hours, and 5.4 hours for cores incubated at 14°C. Comparing between the incubation temperature models, time before anoxic P flux onset was evidently longer across all stations at 8ºC than at 14ºC in summer (ER = 7.46) and fall (ER = 21.6), and similar in spring (ER = 3.50). Among the cores incubated at 14ºC, fall cores tended to have shorter onset than spring or summer, but evidence for this difference was weak. The model for cores incubated at 8°C showed that there was no evidence that onset timing was different across seasons or stations. The onset of anoxic P flux was likely delayed at 8ºC relative to 14°C due to temperature constraints on metabolic oxygen demand which elongated the period of time needed for cores to experience anoxia and for the onset of anoxic P flux to occur. We attribute this delay to temperature dependence of microbial anaerobic respiration that solubilizes iron oxide minerals. Notably, some cores (including all spring CB4 cores) incubated at 8°C never reached anoxia.

Oxic P release rates were higher at 14°C than 8°C during fall (mean difference = 0.51 mg m^{-2} day^{-1}, ER = 26.8) and summer (mean difference = 0.25 mg m^{-2} day^{-1}, ER = 5.18), but similar between the two temperatures in spring (ER = 3.35). Oxic P flux increased as the seasons progressed at 14°C with higher oxic P flux in the fall, but this trend did not occur at 8°C. This trend supports the previous findings that sediments with a history of low-DO exposure experience accelerated P flux sooner. Alternatively, the 8°C cores spent almost a week under oxygenated conditions. This may have been sufficient to ‘reset’ the changes associated with anoxia that made the 14°C cores more susceptible to anoxic P flux onset.

Author Manuscript

Anoxic P flux was not consistently higher at 14ºC than at 8ºC and did not show substantive differences at the level of season or station, but temperature did affect the length of time required for cores to reach anoxia, as onset of anoxic P flux was delayed at 8ºC compared to 14ºC. These temperatures were chosen in order to represent the range of in situ temperatures measured across the seasons (Table 1), but not every temperature and season combination represents realistic in situ conditions. Specifically, the benthos are likely to be closer to 8ºC in spring and closer to 14ºC in fall. The overall estimate for anoxic flux at these times were similar: 11.5±4.3 mg m^{-2} day^{-1} in spring at 8ºC and 11.9±2.2 mg m^{-2} day^{-1} in fall at 14ºC.

Our temperature range caused results to differ from results in previous studies such as Gibbons and Bridgeman (2020) who noted that anoxic P flux was 2-14 times higher at high incubation temperatures (20-30ºC) representing future climate scenarios compared with cores incubated at 10ºC. Our study examined a smaller range of temperatures, 8ºC and 14ºC, and while a larger range of temperatures would be helpful to produce large effects and understand controls on this process, the hypolimnion of the central basin is likely to become anoxic only when temperatures are warm enough to deplete oxygen but cold enough to remain stratified and prevent mixing. Temperature certainly plays a large role in determining the duration of anoxic conditions in the hypolimnion. Specifically, the strong temperature dependence of oxygen consumption means that anoxia will begin earlier and last longer at warmer temperatures.

Author Manuscript

Table 3: Oxic and anoxic P flux and standard errors for cores incubated at 14°C and 8°C and re-aerated anoxic P flux and standard errors are displayed. The different columns correspond to the portions of the experiment denoted in Figure 3. Each release rate represents the mean flux of all cores grouped by season and site that reached anoxia. Seasonal flux means are reported across stations.

P Flux (mg m^{-2} day^{-1}) for Cores Incubated at 14°C and 8°C						
		14°C Core Incubations			**8°C Core Incubations**	
		Oxic Flux	**Anoxic Flux**	**Re-aerated Anoxic Flux**	**Oxic Flux**	**Anoxic Flux**
Spring	**All**	0.39±0.22	13.1±2.25	13.2±6.33	0.21±0.13	11.5±4.32
	CB2	0.37±0.22	10.8±3.49	9.35±5.38	0.35±0.11	9.65±4.67
	CB4	0.41±0.22	17.1±3.38	10.1±5.21	NA	NA
	CB5	0.39±0.22	11.7±2.77	11.4±4.99	0.14±0.09	9.20±4.70
Summer	**All**	0.34±0.23	13.8±2.30	20.2±7.57	0.09±0.13	13.2±4.27
	CB2	0.33±0.24	15.6±2.65	15.9±6.13	0.08±0.12	15.3±5.33
	CB4	0.36±0.25	14.2±2.33	47.0±8.15	0.13±0.13	12.2±6.62
	CB5	0.32±0.23	13.8±2.77	18.2±5.92	0.08±0.14	11.8±5.73
Fall	**All**	0.45±0.25	11.9±2.22	13.1±6.28	-0.06±0.14	15.1±4.06
	CB2	0.44±0.25	11.2±2.40	8.98±5.13	-0.13±0.14	14.8±4.95
	CB4	0.44±0.25	12.3±2.35	12.8±4.92	-0.01±0.13	21.7±7.25
	CB5	0.48±0.25	9.73±2.65	10.6±5.10	-0.11±0.11	14.2±4.02

Figure 4 shows anoxic P flux and standard errors for 14°C incubated cores grouped by site, season, and before and after re-aeration.

Author Manuscript

Figure 4: Anoxic P flux and standard errors for 14°C incubated sediment cores from sites central basin (CB) sites CB2, CB4, and CB5 are shown for the initial and re-aerated portions of this experiment. Core replicates are represented by the smaller, lighter points while flux means are displayed by the larger and darker points.

Methodological limitations and comparisons

The findings from this study may represent an underestimation of sediment P flux as some released P may have been in the form of dissolved organic P (DOP), which we did not measure but can be an important source of P in some systems (Kurek et al., 2021), or was quickly bound or taken up by particles or biomass. We used SRP as the response variable since it captures the principal component forms that are released from sediments under hypoxia. SRP represents multiple component forms of P that are released from sediments under hypoxia, and past studies such as Nürnberg (1988) and Eckert et al. (2020) have found that the ratio of SRP to TP in the hypolimnion after P release approaches 1:1.

Sediment P flux has been measured in lakes across the spectrum of eutrophic and oligotrophic conditions. Nürnberg (1988)'s review of this literature shows that rates determined across system and methodological variance are constrained by a certain bound (range = 0.25 – 51.5 mg m^{-2} day^{-1}, median rate = 10.24 mg m^{-2} day^{-1}). Our findings are in line with the bounds of this worldwide data. Our findings on anoxic P flux and timing from anoxia to anoxic P flux onset are consistent with a companion study that used in situ remote sensing to observe SRP concentration and flux at the hypolimnion of CB2 and CB4 during summer and fall 2019 (Anderson et al., 2021). This remote sensing study produced lag times of 12 - 42 hours and the ensuing anoxic P flux averages ranged from 11.42 - 25.67 mg m^{-2} day^{-1}. This in situ experiment supports the accuracy of this study's short-term sediment coring incubation methodology, which

Author Manuscript

was employed with a focus on high precision through sampling frequency and core replicates across seasons and locations in order to address a gap in our understanding of the environmental conditions, timing, and rates of internal P flux for the central basin.

The scope of this study is limited to the 2019 coring season, and although it shows variation between seasons, it does not account for interannual environmental variability such as anoxic duration or nitrate concentration in the hypolimnion. Hypoxic and anoxic durations are highly affected by environmental factors such as dissolved oxygen consumption rates, temperature, and biomass production. Another factor that may impact interannual variability in anoxia and P loading is the role of nitrate and other alternative electron acceptors that could impact the rate of depletion of dissolved oxygen. Nitrate in the hypolimnion can control P release from sediments as seen in Eckert et al. (2020) who showed that in consecutive years in Lake Kinneret, Israel elevated levels of hypolimnion nitrate delayed and depressed overall P loading relative to the following year with lower hypolimnion nitrate. Additionally, we found no correlations between fluxes and sediment TP (see Supplemental Information), although it remains possible that the mineralogical or chemical conditions led to different amounts of mobile P that our methods did not characterize.

Importance of timing and flux for seasonal loading

Our findings on the timing and rates of sediment P release are relevant when considering the magnitude and effects of basin-wide P loading that occurs seasonally. Yearly variation in the duration of hypoxia and anoxia affects the length and magnitude of basin-wide loading. The rate and timing estimates from our study are based on a single year of observations, but past years of mooring observations can be used to further contextualize the annual durations of these conditions. Hypoxic durations in 2019 were 67 and 43 days at CB2 and CB4 respectively and

Author Manuscript

were 37 and 50 days in 2018 and 17 and 55 days in 2017. Anoxic durations during the 2019 season were 44 and 27 days at CB2 and CB4 respectively, 7 and 23 days during 2018, and 8 and 37 days during 2017 (NOAA NCEI 0210815 and 0210823). 2019 had more hypoxic and anoxic days than the two preceding years, and there is annual variation in the duration of these low DO conditions. In terms of P release rates, this study produced means and ranges of both anoxic and oxic rates. This study found an overall 14°C anoxic P release rate of 12.8 mg m^{-2} day^{-1} across all seasons and stations with a range of 5.19 – 30.7 mg m^{-2} day^{-1}. The 14°C oxic P flux ranged from 0.31 – 0.50 mg m^{-2} day^{-1} with an average of 0.38 mg m^{-2} day^{-1}. The uncertainties in these parameters affect estimates of total basin-wide loading, which has not been calculated here as the spatial extent and duration of anoxia are poorly constrained by existing observations. For example, hypoxia and anoxia begin at the shallow edges of the hypolimnion (Rowe et al., 2019) so the area of sediment responsible for anoxic P flux at any given point in the season will be smaller than the maximum area overlaid by anoxic water at some point during the season. Nonetheless, approximations of total central basin P loading calculations based on release rates are possible (Anderson et al., 2021).

Our findings on delayed onset of anoxic P flux indicate that sediments will not begin accelerated flux until after anoxia has been established. These findings could have a large effect on total basin internal loading estimates within or across years.

Implications for Lake Erie management and monitoring

Internal loading of phosphorus has been cited as a major challenge for long-term P removal and management in water systems (Giles et al., 2015), and monitoring the extent and impact of internal loading will be particularly important as climate change lengthens the duration of stratification (Mason et al. 2016). These conditions will lead to increasingly longer periods of

Author Manuscript

hypolimnion anoxia and higher average P flux (Gibbons and Bridgeman, 2020), both factors that will increase total internal P loads. These future trends make it vital to constrain internal P loading as a function of DO condition and temperature. Expanded and focused monitoring efforts on anoxia and P would help watershed managers and monitoring programs improve our estimates of internal loading and track how it responds to reductions in loading from the watershed.

Internal loading does not add new P to lakes, but rather recycles legacy sediment P from past external loads, which can contribute to and extend hypoxia and anoxia and impact primary production. This stored internal load has the potential to amplify the effects of current external loads depending on the timing, spatial extent, and duration of conditions that favor accelerated release of internal P and vary annually. However, direct observations linking internal loading to enhanced oxygen demand and hypoxia are not available. Sampling campaigns in the central basin typically conclude around the same time as fall turnover, so the fate of the released SRP is uncertain. Winter studies have shown the increasing significance of winter-spring diatom blooms in the central basin, and high carbon flux seen to winter sediments complements this trend, implying that released SRP may have a part in fueling these blooms (Reavie et al., 2016; Wilhelm et al., 2014). Further work in biophysical modeling, specifically a better understanding of spatial hypoxia and anoxia on an annual basis, will be required to constrain interannual differences and predict bioavailable P fate during and after stratification. As the U.S. and Canada pursue further reductions in external loads, it will be important to monitor the extent of anoxia and also monitor the impact on P distribution during and after stratification.

Literature cited

Author Manuscript

Anderson, H.S., Johengen, T.H., Godwin, C.M., Purcell, H., Alsip, P., Ruberg, S., Mason, L. 2021. Continuous *in situ* nutrient analyzers pinpoint the onset and rate of internal P loading under anoxia in Lake Erie's Central Basin. Environ. Sci. Technol. Water. doi: 10.1021/acsestwater.0c00138.

Arega, F., Lee, J.H.W. 2005. Diffusional Mass Transfer at Sediment-Water Interface of Cylindrical Sediment Oxygen Demand Chamber. J. Environ. Eng., 131(5): 755-766. doi: 10.1061/(ASCE)0733-9372(2005)131:5(755).

Beletsky, D., Hawley, N., Rao, Y.R. 2013.Modeling summer circulation and thermal structure of Lake Erie. J. Geophys. Res.: Oceans, 118: 6238-6252. doi: 10.1002/2013JC008854.

Boström, B., Andersen, J.M., Fleischer, S., Jansson, M. 1998. Exchange of phosphorus across the sediment-water interface. Hydrobiol., 170: 229-244.

Bürkner, P. 2018. "Advanced Bayesian Multilevel Modeling with the R Package brms." The R Journal, 10(1): 395–411. doi: 10.32614/RJ-2018-017.

Burns, N.M. and Ross, C. 1972. Project Hypo. CCIW Pap 6 US EPA, Tech Rep TS-05071-208-24.

Caraco, N. 2009. Phosphorus. Reference Module in Earth Systems and Environmental Sciences: Encyclopedia of Inland Waters, 73-78. doi: 10.1016/B978-012370626-3.00097-1.

Author Manuscript

Debroux, J-F., Ceutel, M., Thompson, C., Mulligan, S. 2012. Design and testing of a novel hypolimnetic oxygenation system to improve water quality in Lake Bard, California. Lake and Reservoir Manage., 28: 245-254.

DePinto, J., Young, T., Martin, S. 1981. Algal-Available Phosphorus in Suspended Sediments from Lower Great Lakes Tributaries. J. Great Lakes Res., 7(3): 311-325.

Eckert, W., Beeri-Shlevin, Y., Nishri, A. 2020. Chapter 20: Internal Phosphorus Loading in Sub-tropical Lake Kinneret, Israel, Under Extreme Water Level Fluctuation, p. 377-406. In A.D. Steinman and B.M. Spears [1st ed.], Internal Phosphorus Loading in Lakes: Causes, Case Studies, and Management. J. Ross Publishing.

Edwards, W., Conroy, J., Culver, D. 2005. Hypolimnetic Oxygen Depletion Dynamics in the Central Basin of Lake Erie. J. Great Lakes Res., 31(2): 262-271.

Federal Water Pollution Control Act (Clean Water Act, CWA). 1972. U.S. Government Publishing. https://www.gpo.gov/fdsys/pkg/USCODE-2017-title33/html/USCODE-2017-title33-chap26.htm. Accessed: April 12, 2020.

Foster, S.Q., Fulweiler, R.W. 2019. Estuarine Sediments Exhibit Dynamic and Variable Biogeochemical Responses to Hypoxia. J. Geophys. Res.: Biogeosci., 124. doi: 10.1029/2018JG004663.

Author Manuscript

Gelman, A., Carlin, J.B., Stern, H.S., Rubin, D.B. 2013. Chapter 5: Hierarchical models; Chapter 11: Basics of Markov Chain Simulation. Bayesian Data Analysis. CRC Press LLC.

Gerling, A., Munger, Z., Doubek, J., Hamre, K., Gantzer, P., Little, J., Carey, C. 2016. Whole-Catchment Manipulations of Internal and External Loading Reveal the Sensitivity of a Century-Old Reservoir to Hypoxia. Ecosyst., 19: 555-571.

Giles, C., Isles, P., Manley, T., Xu, Y., Druschel, G., Schroth, A. 2015. The mobility of phosphorus, iron, and manganese through the sediment-water continuum of a shallow eutrophic freshwater lake under stratified and mixed water-column conditions. Biogeochemistry, 127: 15-34.

Gibbons, K.J., Bridgeman, T.B. 2020. Effect of temperature on phosphorus flux from anoxic western Lake Erie sediments, Water Res., doi: 10/1016/j.watres.2020.116022.

Hupfer, M., Lewandowski, J. 2008. Oxygen Controls the Phosphorus Release from Lake Sediments – a Long-Lasting Paradigm in Limnology. Int. Rev. Hydrobiol., 93(4-5): 415-432. doi: 10.1002/iroh.200711054.

Ivey, G.N., Boyce, F.M. 1982. Entrainment by Bottom Currents in Lake Erie. Limnol. Oceanogr., 27(6): 1029-1038.

Author Manuscript

James, W.F. 2012. Estimation of Internal Phosphorus Loading Contributions to the Lake of the Woods, Minnesota. ERDC Report, 42 pp.

Kurek, M.R., Harir, M., Shukle, J.T., Schroth, A.W., Schmitt-Kopplin, P., Druschel, G.K. 2021. Seasonal transformations of dissolved organic matter and organic phosphorus in a polymictic basin: Implications for redox-driven eutrophication. Chem. Geol., 573: 120212.

Lee, J.H.W., Kuang, C.P., Yung, K.S. 2000. Analysis of three-dimensional flow in a cylindrical sediment oxygen demand chamber. Appl. Math. Model., 24: 263-278.

Mason, L., Riseng, C., Gronewold, A., Rutherford, E., Wang, J., Clites, A, Smith, S., McIntyre, P. 2016. Fine-scale spatial variation in ice cover and surface temperature trends across the surface of the Laurentian Great Lakes. Climatic Change, 138: 71-83.

Matisoff, G., Fisher, J.B., Lick, W. 1977. Early Diagenesis and Chemical Mass Transfer in Lake Erie Sediments. US EPA Large Lakes Research Station, Contract No. R805716020.

Matisoff, G., Kaltenberg, E., Steely, R., Hummel, S., Seo, J., Gibbons, K., Bridgeman T., Seo, Y., Behbahani, M., James, W., Johnson, L., Doan, P., Dittrich, M., Evans, M.A., Chaffin, J. 2016. Internal loading of phosphorus in western Lake Erie. J. Great Lakes Res., 42: 775-788.

Author Manuscript

Mohamed, M., Wellen, C., Parsons, C.T., Taylor, W., Arhonditsis, G., Chomicki, K., Boyd, D., Weidman, P., Mundle, S., Van Cappellen, P., Sharpley, A., Haffner, G. 2019. Understanding and managing the re-eutrophication of Lake Erie: Knowledge gaps and research priorities. Freshwater Sci., 38(4): 675-691. doi: 10.1086/705915.

Mortimer, C. 1971. Chemical Exchanges Between Sediments and Water in the Great Lakes-Speculations on Probably Regulatory Mechanisms. Limnol. Oceanogr., 16(2). doi: 10.4319/lo.1971.16.2.0387.

National Oceanic and Atmospheric Administration, Great Lakes Environmental Research Laboratory; Cooperative Institute for Great Lakes Research, University of Michigan. 2020. Water physical, chemical, and biological vertical observational data at multiple levels from fixed mooring CHRP2 and CTD casts taken from NOAA research vessel R5501 in the central basin of Lake Erie, Great Lakes region from 2017-06-09 to 2019-10-10 collected by National Oceanic and Atmospheric Administration, Great Lakes Environmental Research Laboratory and the Cooperative Institute for Great Lakes Research, University of Michigan. (NCEI Accession 0210815). NOAA National Centers for Environmental Information. Dataset. https://accession.nodc.noaa.gov/0210815. Accessed 09/28/2020.

National Oceanic and Atmospheric Administration, Great Lakes Environmental Research Laboratory; Cooperative Institute for Great Lakes Research, University of Michigan. 2020. Water current profile, physical, and chemical vertical observational data at multiple

Author Manuscript

levels from fixed mooring CHRP4 and CTD casts taken from NOAA research vessel R5501 in the central basin of Lake Erie, Great Lakes region from 2017-05-23 to 2019-10-10 collected by National Oceanic and Atmospheric Administration, Great Lakes Environmental Research Laboratory and the Cooperative Institute for Great Lakes Research, University of Michigan. (NCEI Accession 0210823). NOAA National Centers for Environmental Information. Dataset. https://accession.nodc.noaa.gov/0210823. Accessed 09/28/2020.

National Oceanic and Atmospheric Administration, Great Lakes Environmental Research Laboratory; Cooperative Institute for Great Lakes Research, University of Michigan. 2020. Water current profile, physical, and chemical vertical observational data at multiple levels from fixed mooring CHRP5 and CTD casts taken from NOAA research vessel R5501 in the central basin of Lake Erie, Great Lakes region from 2017-05-23 to 2019-10-08 collected by National Oceanic and Atmospheric Administration, Great Lakes Environmental Research Laboratory and the Cooperative Institute for Great Lakes Research, University of Michigan (NCEI Accession 0210822). NOAA National Centers for Environmental Information. Dataset. https://accession.nodc.noaa.gov/0210822. Accessed 09/28/2020.

Nürnberg, G. 1984. The prediction of internal phosphorus load in lakes with anoxic hypolimnia. Limnol. Oceanogr., 29(1): 111-124.

Author Manuscript

Nürnberg, G. 1988. Prediction of phosphorus release rates from total and reductant-soluble phosphorus in anoxic lake sediments. Can. J. Fish. Aquat. Sci., 45: 453-462.

Nürnberg, G. 1991. Phosphorus from internal sources in the Laurentian Great Lakes, and the concept of threshold external load. J. Great Lakes Res., 17(1): 132-140.

Nürnberg, G. 1997. Coping with water quality problems due to hypolimnetic anoxia in Central Ontario Lakes. Water Qual. Res. J. Can., 32: 391-405.

Nürnberg, G., Howell, T., Palmer, M. 2019. Long-term impact of Central Basin hypoxia and internal phosphorus loading on north shore water quality in Lake Erie. Inland Waters, 9(3): 1-12. doi: 10.1080/20442041.2019.1568072.

Paytan, A., Roberts, K., Watson, S., Peek, S., Chuang, P-C., Defforey, D., Kendall, C. 2017. Internal loading of phosphate in Lake Erie Central Basin. Sci. Total Environ., 579: 1356-1365.

Phillips, G., Kelly, A., Pitt, J-A., Spears, B.M. 2020. Chapter 13: Barton Broad, UK: Over 40 Years of Phosphorus Dynamics in a Shallow Lake Subject to Catchment Load Reduction and Sediment Removal, p. 243-262. In A.D. Steinman and B.M. Spears [1st ed.], Internal Phosphorus Loading in Lakes: Causes, Case Studies, and Management. J. Ross Publishing.

Author Manuscript

Reavie, E., Cai, M., Twiss, M., Carrick, H., Davis, T., Johengen, T., Gossiaux, D., Smith, D., Palladino, D., Burtner, A., Sgro, G. 2016. Winter-spring diatom production in Lake Erie is an important driver of summer hypoxia. J. Great Lakes Res., 42(3): 608-618.

Rowe, M., Anderson, E., Beletsky, D., Stow, C., Moegling, S., Chaffin, J., May, J., Collingsworth, P., Jabbari, A., Ackerman, J. 2019. Coastal Upwelling Influences Hypoxia Spatial Patterns and Nearshore Dynamics in Lake Erie. J. Geophys. Res.: Oceans, 124(8): 6154-6175. doi: 10.1029/2019JC015192.

Rowland, F., Stow, C., Johengen, T., Burtner, A., Palladino, D., Gossiaux, D., Davis, W., Johnson, L., Ruberg, S. 2020. Recent Patterns in Lake Erie Phosphorus and Chlorophyll *a* Concentrations in Response to Changing Loads. Environ. Sci. Technol., 54: 835-841.

Ruberg, S., Guasp, E., Hawley, N., Muzzi, R., Brandt, S., Vanderploeg, H., Lane, J., Miller, T. 2008. Societal Benefits of the Real-Time Coastal Observation Network (ReCON): Implications for Municipal Drinking Water Quality. Mar. Technol. Soc. J., 42(3): 103-109.

Scavia, D., David Allan, J., Arend, K. K., Bartell, S., Beletsky, D., Bosch, N. S., Brandt, S.B., Briland, R., Daloğlu, I., DePinto, J., Dolan, D., Evans, M.A., Farmer, T., Goto, D., Han, H., Höök, T., Knight, R., Ludsin, S., Mason, D., Michalak, A., Richards, P., Roberts, J., Rucinski, D., Rutherford, E., Schwab, D., Sesterhenn, T., Zhang, H., Zhou, Y. 2014.

Author Manuscript

Assessing and addressing the re-eutrophication of Lake Erie: Central basin hypoxia. J. Great Lakes Res., 40(2): 226-246. doi: 10.1016/j.jglr.2014.02.004.

Scavia, D., Bertani, I., Obenour, D.R., Turner, R.E., Forrest, D.R., Katin, A. 2017a. Ensemble modeling informs hypoxia management in the northern Gulf of Mexico. PNAS, 114: 8823-8828.

Scavia, D., Kalcic, M., Muenich, R. L., Read, J., Aloysius, N., Bertani, I., Boles, C., Confesor, R., DePinto, J., Gildow, M., Martin, J., Redder, T., Robertson, D., Sowa, S., Want, Y., Yen, H. 2017b. Multiple models guide strategies for agricultural nutrient reductions. Front. Ecol. Environ., 15(3): 126-132.

Seal AA3 AutoAnalyzer Manual. Method No. G-297-03 Rev. 5 (Multitest MT 19).

Snodgrass, W., Fay, L. 1987. Values of Sediment Oxygen Demand Measured in the Central Basin of Lake Erie, 1979. J. Great Lakes Res., 13(4): 724-730.

Stan Development Team. 2020. RStan: the R interface to Stan. R package version 2.21.2. http://mc-stan.org/.

Steinman, A.D., Spears, B.M. 2020. Chapter 1: What Is Internal Phosphorus and Why Does It Occur?, p. 3-14. In A.D. Steinman and B.M. Spears [1st ed.], Internal Phosphorus Loading in Lakes: Causes, Case Studies, and Management. J. Ross Publishing.

Author Manuscript

Stone, J.P., Pangle, K.L., Pothoven, S.A., Vanderploeg, H.A., Brandt, S.B., Höök, T.O., Johenged, T.H., Ludsin, S.A. 2020. Hypoxia's impact on pelagic fish populations in Lake Erie: a tale of two planktivores. Can. J. Fish. Aquat. Sci., 18: 1-18. doi: 10.1139/cjfas-2019-0265.

Vahtera, E., Conley, D., Gustafsson, B., Kuosa, H., Pitkänan, H., Savchuk, O., Tamminen, T., Voss, M., Wasmund, N., Wulff, F. 2007. Internal Exosystem Feedbacks Enhance Nitrogen-fixing Cyanobacteria Blooms and Complicate Management in the Baltic Sea. Ambio., 36(2/3): 186-194.

Wilhelm, S. W., G. R. LeCleir, G. S. Bullerjahn, R. M. McKay, M. A. Saxton, M. R. Twiss, and R. A. Bourbonniere. 2014. Seasonal changes in microbial community structure and activity imply winter production is linked to summer hypoxia in a large lake. FEMS Microbiol. Ecol., 87: 475-485.

Zhang, H., Boegman, L., Scavia, D., Culver, D.A. 2016. Spatial distributions of external and internal phosphorus loads in Lake Erie and their impacts on phytoplankton and water quality. J. Great Lakes Res., 42(6): 1212-1227. doi: 10.1016/j.jglr.2016.09.005.

Zhou, Y., Obenour, D., Scavia, D., Johengen, T., Michalak, A. 2013. Spatial and Temporal Trends in Lake Erie Hypoxia, 1987-2007. Environ. Sci. Technol., 47: 899-905.

Zorn, M., Waples, J., Valenta, T., Kennedy, J., Klump, J.V. 2018. *In situ*, high-resolution time series of dissolved phosphate in Green Bay, Lake Michigan. J. Great Lakes Res., 44: 875-882.

Author Manuscript

Author Manuscript

Acknowledgements:

This work was supported by the National Oceanic and Atmospheric Administration's National Centers for Coastal Ocean Science Competitive Research Program under award NA16NOS4780209 to the University of Michigan, the Great Lakes Restoration Initiative (GLRI), Cooperative Science and Monitoring Initiative (CSMI), and through the NOAA Cooperative Agreement with the Cooperative Institute for Great Lakes Research (CIGLR) at the University of Michigan (NA17OAR4320152). This is CIGLR contribution no. 1183 and CHRP contribution no. 256. This work was supported by vessel crew Daniel Burlingame, Todd Roteman, and Kent Baker. Ashley Burtner assisted with measuring phosphorus samples. Lacey Mason produced Figure 1. Three reviewers provided comments on this manuscript which greatly improved the quality and clarity of our study.

No conflicts of interest were reported for this study. Data and R code is available upon request to the corresponding author.

Author Manuscript

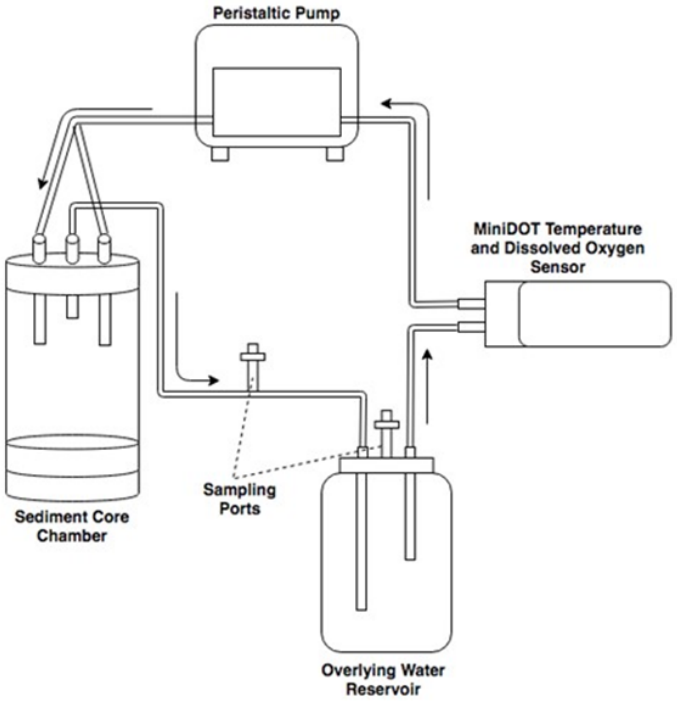

Author Manuscript

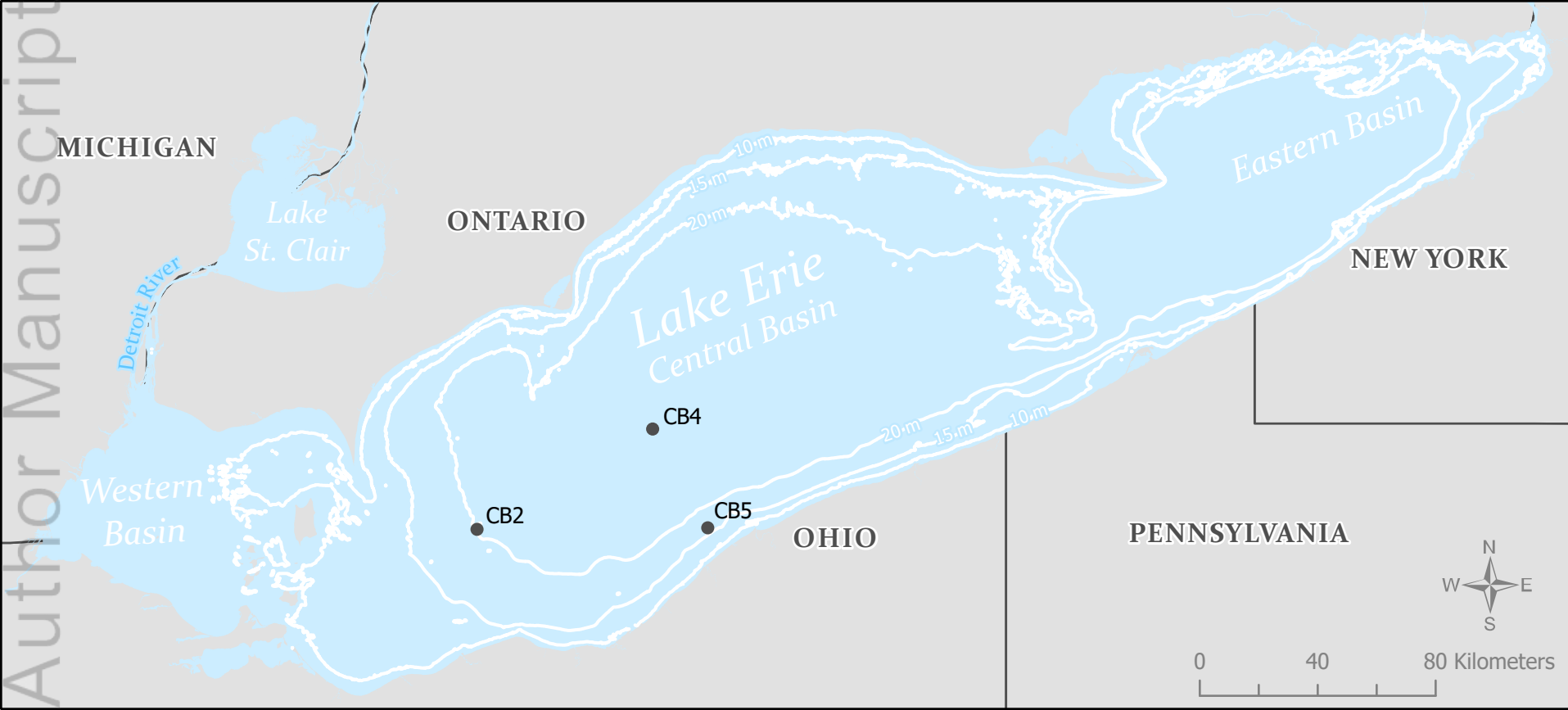

Author Manuscript

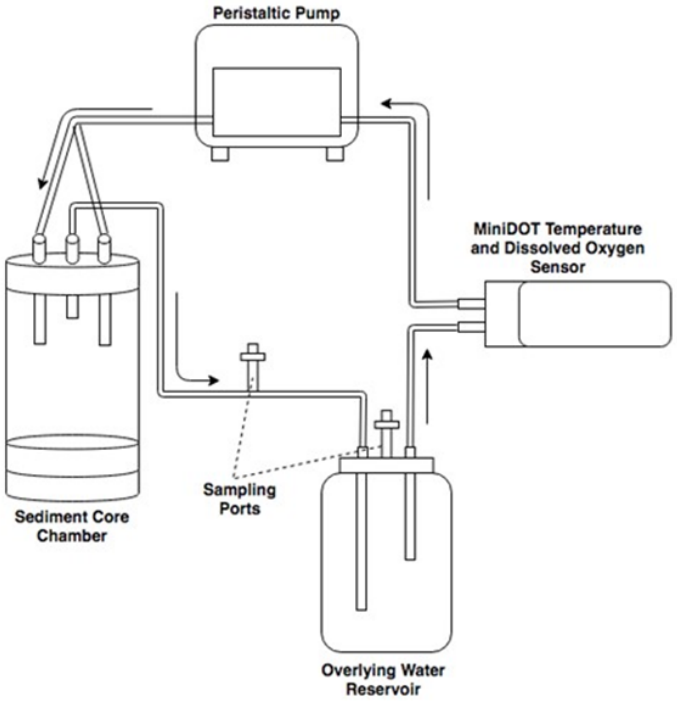

Author Manuscript

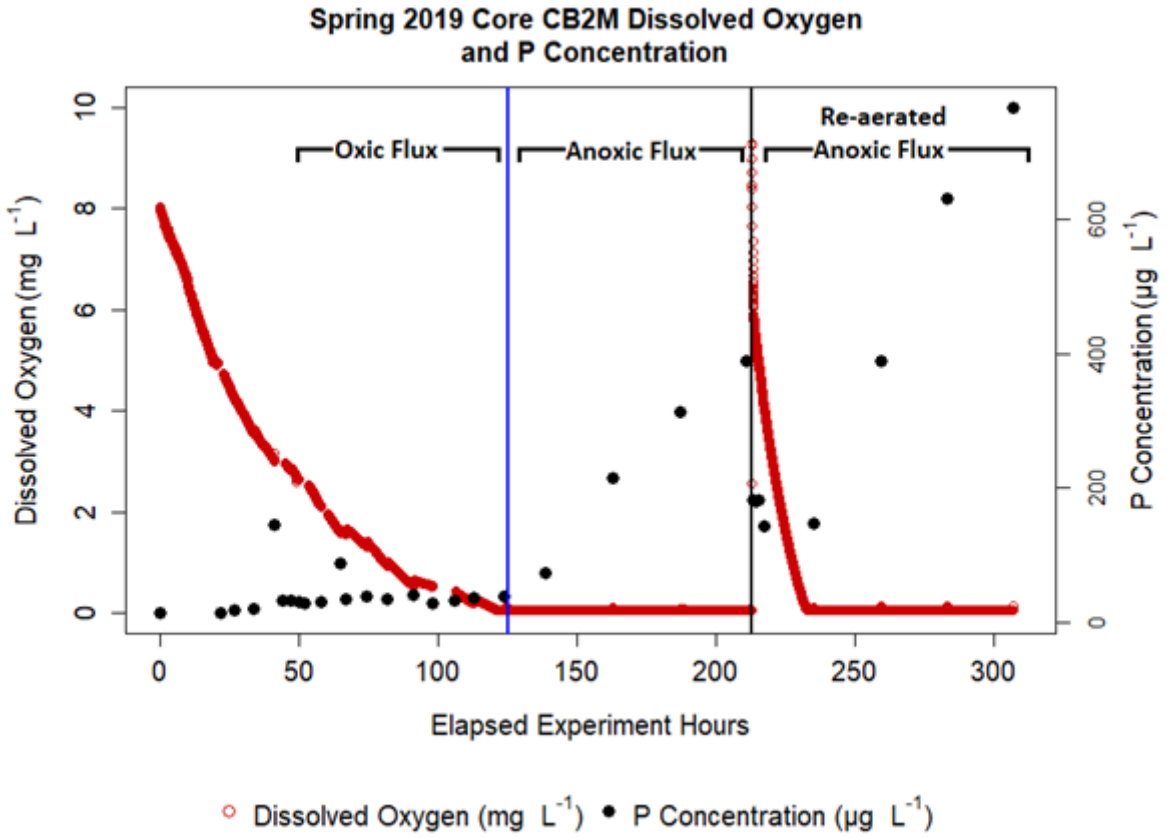

LNO_11900_Figure 3.tif

Author Manuscript

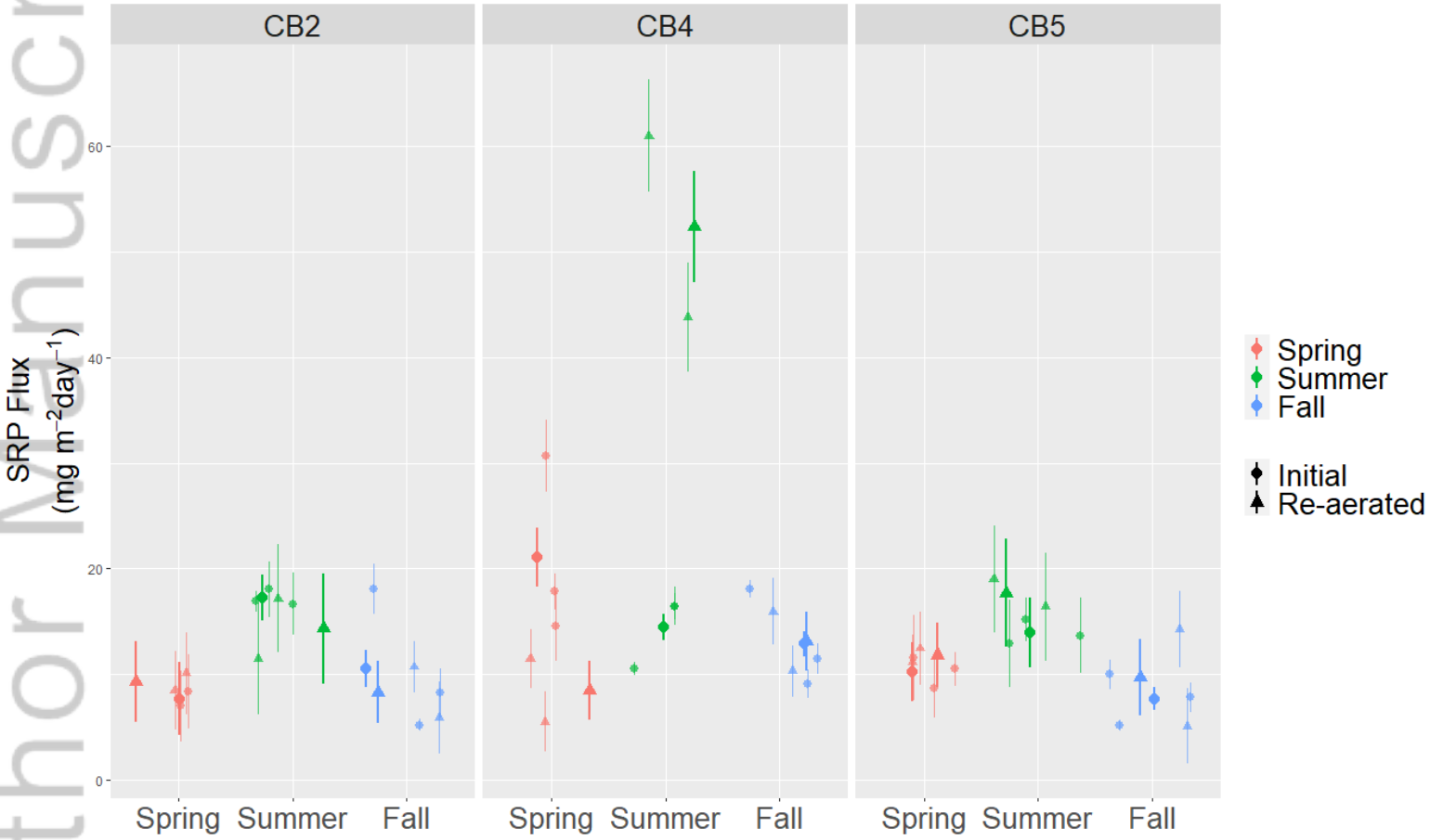

LNO_11900_Figure 4.tiff

Accelerated sediment phosphorus release in Lake Erie's central basin during seasonal anoxia

Hanna S. Anderson[1*], Thomas H. Johengen[1], Russ Miller[1,] and Casey M. Godwin[1]

*Corresponding author: Hanna S. Anderson, hannaand@umich.edu

[1]Cooperative Institute for Great Lakes Research (CIGLR), School for Environment and Sustainability, University of Michigan, Ann Arbor, MI, USA

Author email addresses: Hanna S. Anderson, hannaand@umich.edu; Thomas H. Johengen, johengen@umich.edu; Russ Miller, rusmil@umich.edu; Casey M. Godwin, cgodwin@umich.edu

Key words: Lake Erie, internal phosphorus loading, phosphorus sediment flux, anoxia, eutrophication

Author Manuscript

Abstract

Eutrophication remains a serious threat to Lake Erie and has accelerated over past decades due to human activity in the watershed. Internal phosphorus (P) loading from lake sediment contributes to eutrophication, but our understanding of this process in Lake Erie is more uncertain than for its riverine P inputs. Past work has focused on incubating sediment cores in oxic or anoxic conditions, meaning we know little about sediment flux during state transitions. We used fifty-six controlled sediment core incubation experiments to quantify rates and onset of P release in Lake Erie's central basin as a function of depositional environment, season (spring, summer, and fall), temperature, and dissolved oxygen (DO) concentration. P flux under oxic or hypoxic (>0 to ≤2 mg L^{-1} DO) conditions was slow (0.31 – 0.50 mg m^{-2} day^{-1}) compared to anoxic P flux (5.19 – 30.7 mg m^{-2} day^{-1}). The transition between slow and fast flux occurred within 24 hours of anoxia (0 mg L^{-1} DO). Oxic or anoxic P flux was generally similar across seasons and incubation temperatures (8 and 14ºC). In 14°C incubated cores anoxic P flux onset was earliest in fall, when sediments had already been exposed to anoxic conditions in the lake. Re-oxygenation of experimental cores that temporarily developed anoxia reversed the direction of P flux, but P release resumed at similar rates once the water returned to anoxia. Understanding the effects of hypolimnion oxygen conditions on internal P loading allows us to better constrain nutrients sources and implications for P budget management.

Author Manuscript

Introduction

Lake Erie has a history of environmental degradation, and past industrial and wastewater runoff led to eutrophication throughout the lake (DePinto et al., 1981). Consequences of eutrophication have included promotion of harmful algal blooms (HABs) in the western basin and summertime hypoxia in the central basin. Environmental regulations such as the U.S. Clean Water Act (CWA, 1972) forced the management of point source pollution, and many of the ecological consequences of pollution were diminished or abated for a time (Scavia et al., 2014). Despite recent management efforts targeting point source nutrient pollution from Lake Erie's watershed, both HABs and hypoxia remain problems for the lake (Scavia et al., 2014), in part due to continued land use changes and agricultural practices. In Lake Erie and other aquatic environments, hypoxia changes food web structures, biogeochemical cycling in the water and sediment, habitat availability, and life cycles of key species (Stone et al., 2020; Foster and Fulweiler, 2019). The spatial extent of hypoxia and anoxia (0 mg L^{-1} DO) in Lake Erie within a given year is dependent on thermal structure and the timing of stratification (Beletsky et al., 2013), hydrodynamic movements (Rowe et al., 2019), and wind stress. Over longer timescales, studies have shown that hypoxia in the central basin is related to, and has recently expanded in response to, increased tributary P discharge (Zhou et al., 2013; Edwards et al., 2005). Nutrient loading reductions are prioritized as a means to minimize hypoxia and other symptoms of eutrophication, and although interannual variability in P loading is well understood in the western basin (Matisoff et al., 2016; Scavia et al., 2017b; Rowland, et al., 2020), improved characterization of P loading and sources is needed for the central basin (Mohamed, 2019).

Another input of nutrients comes from the recycling of legacy P inputs stored in lake sediments via internal phosphorus loading, a potentially important component of a lake's P

Author Manuscript

budget (Nürnberg, 1984; Nürnberg, 1991). A major driver of internal P loading occurs when low dissolved oxygen (DO) conditions and redox conditions at the sediment-water interface allow for inorganic P to flux out of the sediment (Foster and Fulweiler, 2019). Eutrophication can exacerbate internal loading as excess growth of algal biomass can later fuel increased oxygen consumption in the hypolimnion. Decaying organic matter from algal blooms is remineralized as it integrates into lake sediment, creating a reservoir of nutrients over time (Gerling et al., 2016) and driving respiration of dissolved oxygen (Reavie et al., 2016). Under oxic conditions, iron oxides (such as Fe III oxyhydroxides) are powerful sorbents of inorganic phosphorus (Davidson, 1993) but when DO is absent, microbes respire these oxides and convert them to a soluble form that releases bound inorganic P (Boström et al., 1998; Mortimer, 1971). This results in internal phosphorus flux as inorganic P diffuses into the water (Steinman and Spears, 2020). This effect, known as "accelerated eutrophication", has been suggested for various water bodies (Caraco, 2009; Vahtera et al., 2007) and can act as a positive feedback mechanism that complicates efforts to control eutrophication through limiting loading from the watershed (Steinman and Spears, 2020). Although this mechanism is well recognized, there is uncertainty as to the relationship between watershed loading of P and hypoxic extent in the central basin of Lake Erie (Scavia et al., 2017a).

The morphological and physical conditions of Lake Erie's central basin make it especially susceptible to widespread anoxia and internal phosphorus loading compared to other large lakes. In the central basin (max depth 25 m) seasonal thermal stratification and basin morphology yield a warm, thin hypolimnion often only 2-3 meters thick. Organic matter production in the basin creates high oxygen demand and adds a large supply of nutrients to the surface sediment, leading to recurring seasonal hypoxia and anoxia. Lake Erie has specific areas

Author Manuscript

that are spatially and temporally vulnerable to hypoxia and anoxia, including the Ohio shoreline of the central basin (Rowe et al., 2019). Lake Erie's large-scale occurrence of low DO conditions and internal loading makes it an important system in which to study these processes.

There are a few recent experimental measurements of internal P loading for the central basin, but available estimates show highly divergent rates. Matisoff et al. (1977) performed a sediment core incubation study and found anoxic P flux from 12.8 to 73.5 mg m^{-2} day^{-1} at 14-16°C. More recently, Paytan et al. (2017) incubated central basin sediment cores at 7°C and calculated anoxic P flux as 0.32 mg m^{-2} day^{-1} and oxic P flux at 0.58 mg m^{-2} day^{-1}. Paytan's incubation experiment occurred after cores were stored for a 2-month period which, combined with a relatively low incubation temperature, may explain the difference in this anoxic P flux estimate relative to others. Nürnberg et al. (2019) presented a different approach that combined summer water collection data showing TP increases over 9 years, in situ hypolimnion P concentration change data from Burns and Ross (1972), and total surface sediment P concentrations from an earlier study (Nürnberg, 1988), which estimated hypoxic P flux at 7.6-8 mg m^{-2} day^{-1}.

In addition to the limited number of measurements of P flux from Lake Erie, there is also a lack of consensus regarding the conditions that result in accelerated P flux. Some models assume that accelerated flux begins at varying definitions of anoxia, some at 1.0 mg DO L^{-1} and others at 1.5 mg DO L^{-1} (Zhang et al., 2016). Since estimates of internal loading are critically dependent on the area and duration of sediments that are undergoing accelerated P flux, we need to understand precisely the DO conditions that lead to flux. Pinpointing these conditions is especially important in Lake Erie, where hypoxia and anoxia exhibit dramatic inter-annual variability (Zhou et al., 2013), and advection or upwelling can disrupt stratification and

Author Manuscript

hypolimnion anoxia, causing abrupt changes in the redox condition at the sediment-water interface (Ruberg et al., 2008). Detailed continuous monitoring in Green Bay, Lake Michigan by Zorn et al. (2018) showed that turnover events and subsequent re-stratification had mixed effects on hypolimnion phosphorus concentration and DO consumption during organic matter remineralization, but the effects on P flux were not fully characterized. Our study mimics re-stratification events in experimental cores in order to observe and replicate the conditions and rates of P release in response to short-term disruptions of the hypolimnion at a fine scale. To complement this incubated sediment core study, we also performed continuous in situ monitoring in Lake Erie's central basin where we monitored a hypolimnion disruption event and observed that average P flux was higher after this disturbance than before (Anderson et al., 2021).

Our study used a series of controlled sediment core incubations to quantify: 1) oxygen conditions required for the onset of P flux, 2) rates and timing of phosphorus flux with respect to location in Lake Erie's central basin, temperature, time of year, and DO conditions, and 3) behavior of P flux following a hypolimnion-disturbing event.

Materials and methods

We sampled sediment cores at three locations in Lake Erie's central basin in order to represent differing depositional environments (Figure 1). These locations were each adjacent to instrumented moorings that continuously recorded temperature and dissolved oxygen throughout the water column. Sediment coring at site CB5 took place several kilometers offshore from the site due to non-depositional and uncoreable substrate at the mooring location. Detailed descriptions of the locations and environmental context of the moorings are available in the NOAA National Centers for Environmental Informatics (NCEI, www.ncei.noaa.gov) under

Author Manuscript

Accession numbers 0210815, 0210823; and 0210822. Coring experiments were performed during spring (June 4-5), summer (July 24-25), and fall (September 18-19) of 2019.

Figure 1: Map of Lake Erie including the three central basin (CB) coring sites. The three depth contour lines represent water column depths of 10, 15, and 20m.

Each season, cores were collected over a span of 2 days, with all cores from a single site collected at the same time. An Ekman box corer (30 x 30 cm) was used to retrieve large, undisturbed sediment samples (>0.5 m thickness) and overlying hypolimnion water from each site. Experimental cores were manually collected from the box core using polycarbonate cores with a total length of 30.5 cm and diameter of 14.6 cm. Only one experimental core was extracted from each box core due to disturbance of the sediment surface during collection. Each core contained an average of 2,130 cubic cm of sediment and 1,723 mL of overlying hypolimnion water. The experimental cores were based on the design of Arega and Lee (2005) and were sealed at the top with an air-tight core lid (details below) and an expanding plug below the sediments. In addition to the experimental cores, a small 3 cm diameter core was collected from each box core, from which we extruded and froze the top 1 cm for elemental analyses (methods and results available in Supplemental Information).

During each sampling event, 100 L of hypolimnion water was collected using a submersible pump coupled to a water quality sonde (YSI EXO2 Multiparameter Sonde) to monitor collection conditions. This water was used as overlying water during sediment core incubations. A small sample of this overlying water was filtered and analyzed for soluble reactive phosphorus (SRP) concentration as described below. The lake was not strongly stratified for the June collection, so water was collected 4-5 m from the bottom. At each sampling site, care was taken to avoid collecting water from areas where the hypolimnion was disturbed by

Author Manuscript

sediment coring. Table 1 lists ambient lake water temperature, dissolved oxygen, conductivity, and pH at the time of each sampling. Exact sediment coring depths varied between seasons due to lake bathymetry, but were approximately 21.5 m at CB2, 24.5 m at CB4, and 22 m at CB5. After collection, experimental sediment cores and water samples were transported to the Great Lakes Environmental Research Laboratory (GLERL) in Ann Arbor, MI. The cores remained sealed, shielded from light, and cooled with ice for the average 8 hours of transport time from collection to laboratory.

Author Manuscript

Table 1: Summary of 2019 coring dates and locations with accompanying sonde data.

		Date Cored	Water Sampling Depth (m)	Bottom Temp (°C)	Bottom Dissolved Oxygen (mg L^{-1})	Hypolimnion SRP (µg L^{-1})	Conductivity (µS cm^{-1})	pH
Spring	**CB2**	**June 4**	15.0	12.5	10.3	0.96	255	7.98
	CB4	**June 5**	20.5	8.10	9.50	2.11	268	7.67
	CB5	**June 5**	21.6	8.30	9.80	2.32	267	7.71
Summer	**CB2**	**July 25**	20.8	12.4	5.40	2.92	284	7.50
	CB4	**July 24**	23.6	8.50	6.34	3.32	279	7.45
	CB5	**July 24**	22.8	10.4	6.56	4.54	277	7.57
Fall	**CB2**	**Sep. 19**	16.6	12.3	0.07	36.6	279	7.71
	CB4	**Sep. 18**	23.8	11.0	0.02	34.2	283	7.08
	CB5	**Sep. 18**	21.1	12.0	0.02	28.1	278	7.33

Sediment core chambers were designed as closed circulation systems (Figure 2) (Arega and Lee, 2005). The design and hydraulics of this core incubation setup were shown to be useful for observing exchange processes across the sediment-water interface (Arega and Lee, 2005; Lee et al., 2000). Core chambers had one central output and two input jets for water circulation, all located at the top of the core. The circulation systems consisted of 3.12 mm tubing (Cole-Parmer EW-06440-16) connecting the sediment core, a reservoir, and a dissolved oxygen sensor (PME MiniDOT) with flow-through adapter to a peristaltic pump (see Figure 2). Airtight compression fittings were used to connect the tubing to the incubated cores to prevent gas exchange. Sampling ports associated with each core allowed us to sample overlying water throughout the incubation period, and input and withdrawal ports were physically separated within the flow system to prevent short-circuit uptake in the withdrawn sample. In order to prevent readings in stagnant

Author Manuscript

water, which is problematic for optical DO sensors, we built flow cells to ensure the DO sensors were exposed to high-velocity water in the circulation system. One potential shortcoming of this experimental setup is that the reservoirs and circulation system may create micro-environments that are slightly different from the overlying water in the core. While the water circulation ensured that these volumes were well-mixed, small differences in the oxygen concentration between the sensor sediment surface may slightly impact our estimates of the dissolved oxygen concentration at which accelerated P flux begins.

On each date (Table 1) we collected 6 cores from each sampling station. We randomly divided the cores from each site into triplicates incubated at 8ºC and triplicates incubated at 14ºC. Among the three stations, this yielded a total of 9 cores incubated at 8ºC and 9 cores incubated at 14ºC during each season. Cores from each season were incubated at both temperatures in order to control for seasonality and temperature variables, although not every temperature and season combination represents realistic in situ conditions. In particular, the temperature of the hypolimnion in summer (July) is likely more variable than the other seasons and depends on location within the basin and water circulation (Rowe et al., 2019). All 9 cores at each temperature were incubated in a common, darkened environmental chamber. Each core had a separate reservoir, DO sensor, and tubing. Flow was maintained by multichannel peristaltic pumps, each of which controlled 3 or 4 cores.

Figure 2: Diagram of the core incubation system used for the experiments. Components include sediment core chamber, peristaltic pump, overlying water reservoir, dissolved oxygen sensor, and connective tubing with sampling ports. Arrows indicate direction of water flow.

Upon return to the laboratory, cores were placed within the incubators and allowed to settle for 30 minutes. Each incubator contained 9 cores, three from each coring site. Stainless

Author Manuscript

192 steel jets that allowed circulating water to enter the sediment core chamber were adjusted so that
193 the outlets were fixed approximately 3-4 cm above the sediment pointing in opposite directions
194 to create well-mixed conditions with velocities of ~1-3 cm s^{-1} that approximated the
195 predominantly horizontal water velocities expected near the sediment surface without disturbing
196 the sediment and causing release of P due to high water velocity (Lee et al., 2000; Arega and
197 Lee, 2005; Ivey and Boyce, 1982). After settling, the cores were flushed with unfiltered site
198 water (containing all the biota naturally present in the hypolimnion) sampled at the time of
199 coring to replace the original water from the system and minimize the effects of any disturbed
200 sediment from transport in order to start with fully oxygenated conditions. After the flushing
201 process, we began a period of open circulation during which the unfiltered overlying water was
202 re-circulated through an open bath inside the incubator. This open circulation was intended to
203 ensure that overlying water was saturated with DO prior to sampling. The peristaltic pumps
204 operated at 125 mL min^{-1} during the 60-minute flushing process and the 8-hour open exchange.
205 Closed circulation began when the reservoir output tube was attached to the input of the
206 DO sensor and the sensor was removed from the bath. Each sediment core incubation system
207 was checked for air bubbles. To displace any headspace remaining in the components,
208 replacement overlying water was added via the input port. Circulation rates during the
209 experiment were set based on the chamber design paper (Arega and Lee, 2005) to mimic
210 published accounts of lake bottom conditions (Snodgrass et al., 1987) with the goal of not
211 disturbing the sediment-water interface. During the first 24 hours of closed circulation when DO
212 was > 4 mg L^{-1}, peristaltic pump speeds were varied every few hours between 50, 125, and 250
213 mL min^{-1} as an experimental variable to examine flow rate effect on sediment oxygen demand
214 rates (Arega and Lee, 2005). Following this period, and when DO was still > 3 mg L^{-1}, pump

Author Manuscript

speeds were maintained at a fixed rate of 125 mL min^{-1} for the remainder of the experiment including the transition to anoxia.

During incubation, dissolved oxygen and temperature were recorded every 60 seconds and water samples for SRP concentration were taken at discrete time points (6-24 hour intervals) over the course of the incubation in order to capture P flux behavior across the range of DO conditions. We assumed steady-state DO condition throughout the system. Although it is possible that the sediments reached anoxia before the overlying water was completely anoxic, we aimed to quantify the onset with respect to dissolved oxygen in the water, which is more readily and frequently monitored than sediment conditions. Core water samples were collected using syringes via the sampling port system at least once every 24 hours while DO consumption rates were low, and more frequently when core water approached hypoxic conditions (2 mg L^{-1} DO). To collect each sample, 45 mL of water was removed through one port while an equal amount of temperature-equilibrated overlying water was added back via the second port with another syringe. Water samples were immediately filtered into test tubes from collection syringes using membrane filters with a 0.2 µm pore size and frozen at -20ºC until analysis. Total incubation length ranged from 12-16 days, with variation between seasons based on the amount of time needed for complete depletion of dissolved oxygen.

Following at least 4 days of sustained anoxia, a subset of cores incubated at 14ºC were re-aerated in order to observe how sediment P flux responded to conditions of short-term replacement of local anoxic water with normoxic water. We did not perform replacements for the 8ºC cores as they generally took much longer to reach anoxia, and such long incubation times eventually decreased the efficacy of the incubation systems. The purpose of re-aeration was to mimic replacements of hypolimnetic water, which have been observed in Lake Erie (Ruberg et

Author Manuscript

al., 2008). This re-aeration experiment was repeated in the spring, summer, and fall and involved replacing the overlying incubation water from selected core replicates with oxygenated hypolimnion water collected from each site. The average SRP concentrations from the 14°C re-aerated core overlying water before and after re-aeration were 232.1 µg L^{-1} and 43.3 µg L^{-1}. This means that while the volume of the cores remained the same, the sediment-water concentration gradient dropped so that flux would not be gradient-limited following re-aeration. This water replacement was slow enough as to not disturb the sediment and expose a new surface to the new overlying water. The re-aeration experiment was performed in 2 of the 3 cores from each sampling location while the third core was left undisturbed. This re-aeration experiment mimics sudden replacements of overlying water with some caveats. The sediment cores are volume-limited, meaning SRP accumulates in the fixed overlying water volume, causing the sediment-water concentration gradient to become more severe. This limits P release from surface sediments after prolonged incubation relative to the natural system. Additionally, the re-aeration experiment does not re-establish the depth of oxic penetration in the sediment that was present before coring, so the second P flux may happen earlier than in an in situ re-aeration scenario with longer re-exposure to oxic conditions. These nuances are reflective of the variations of in situ hydrodynamic movements that lead to anoxic water being rapidly replaced with oxic water.

Samples from both the sediment cores and the original overlying water were analyzed for soluble reactive phosphorus (SRP) using a Seal AA3 auto-analyzer using the molybdate blue reaction (Method No. G-297-03 Rev. 5 Multitest MT 19). SRP standards were prepared daily from a NIST-traceable stock (Hach Company). Preliminary experiments revealed that anoxic water could cause matrix effects with this analytical method, possibly due to co-elution of dissolved iron from sediments, so samples were diluted with deionized water at a range of

Author Manuscript

concentrations. All samples were run in duplicate and the median relative standard deviation among replicates was 2.01%. The analytical detection limit was 1 µg L^{-1}, and diluted samples had proportionally higher detection limits. Several samples were below detection limits, and these were primarily immediately following re-aeration and were omitted from the regressions. This study focuses on release of soluble reactive P and therefore all reported P flux estimates refer to phosphorus in the form of SRP.

P flux from sediment to water was calculated using the change in concentration of SRP in water over time. We estimated this rate in two or three different phases in each core, shown in Figure 3. Similar to previous work (Anderson et al., 2021), we did not find accelerated increases in SRP until close to or after the onset of anoxia. To account for the dilution or addition of P due to each sampling and water replacement (on average 1.2% of the total overlying volume), we estimated the cumulative total P released from the sediment at each timestep using Equation 1.

Equation 1: $$m_t = m_{t-1} + v_{total}(c_t - (c_{t-1} \times \frac{V_{total} - V_{removed}}{V_{total}} + c_{OLW} \times \frac{V_{removed}}{V_{total}}))$$

In Equation 1, m_t and m_{t-1} are accumulated masses of P in the water (mg P per core), c_t is the concentration at time t, c_{t-1} is the concentration measured at the previous time point, c_{OLW} is the concentration of P in the overlying water that was added when a sample was removed, V_{total} is the total water volume in the incubation system, and $V_{removed}$ is the volume of water removed from the system at each sampling time point. We performed this adjustment calculation for each timestep except for the re-aeration events, where we used the first measurement following water replacement for the first timepoint.

The P accumulation data was used to calculate P release rates from the sediment during normoxic and anoxic conditions. We set the timescale for each core to begin (t = 0) at the onset of anoxia based on each core's DO data. This allowed us to express the timing of flux

Author Manuscript

acceleration with respect to the onset of anoxia without affecting the rates found during oxic or anoxic conditions. In order to estimate both rates and the transition time at which the flux accelerates (the onset timing), we fitted segmented linear regressions to accumulated P versus time elapsed. Throughout this paper, this accelerated flux under anoxia is termed anoxic P flux. Only anoxic P rates were calculated during re-aeration as rapid DO consumption under these conditions made it difficult to fit reliable oxic P rates.

Onset of anoxic P flux was calculated relative to the time when each core first experienced anoxic conditions. Conventional definitions of anoxia as a nominal zero DO concentration and noted experimentally by minimum DO readings for each sensor (with a range of 0.007-0.020 mg L^{-1}), were used as the indication for anoxia onset during incubation. This lower limit was determined by incubating all sensors in water dosed with potassium meta-bisulfite where anoxia was confirmed with Winkler titrations. Anoxic P flux onset (hours) was calculated as the difference between the time of the last dissolved oxygen measurement above anoxia and the transition time to anoxic P flux in each incubating core. While sampling was done at regular intervals during the transition to anoxia, in some cases lower sampling frequency led to increased uncertainties in the estimations of transition time to anoxic P flux. Sampling frequency was increased during the re-aeration experiment in order to capture faster expected P flux, and although this increased accuracy for this part of the experiment, it introduced a possible source of error in terms of sampling rate bias relative to the initial portion of the experiment.

In order to derive estimates of rates and timing from all of the available data, we fit the segmented regressions using a hierarchical Bayesian framework. This approach is similar to a mixed-effects regression model, with fixed effects and random effects for each replicate, but has the advantage of using all the information to help constrain estimates at the innermost level (e.g.,

Author Manuscript

individual cores or replicates from the same season and station) without requiring interaction terms. All analyses were performed in R (Version 4.0.2) using the package "brms" (Bürkner, 2018) to compile Bayesian regression models that were fitted using a Hamiltonian Markov Chain Monte Carlo algorithm in "stan" (Stan Development Team, 2020). Anoxic P flux calculations were constrained to the four days immediately following anoxia to avoid incorporating slower rates and other artifacts that occur after extended periods of anoxia in the volume-limited sediment cores. We made separate models for cores incubated at 8°C, cores incubated at 14°C prior to the re-aeration experiment, and cores incubated at 14°C during the re-aeration experiment. Within each hierarchical regression the outermost grouping term was season followed by station and core. Both the slopes and intercepts were allowed to vary among each level of the hierarchy.

We calculated the mean, standard errors, and credible intervals (95%) for each model parameter using the posterior distribution. Estimates from the posterior distribution represent the deviation from the overall mean rate. Each regression was informed by four Markov chains and weakly informative priors for the oxic P flux (location = 0, standard deviation =10), the transition time (10, 5) and the anoxic P flux (0, 10). After 1000 warmup iterations, each chain was sampled for 1000 iterations. We assessed that the cores had converged using the Gelman-Rubin statistic, which was $\hat{R} < 1.01$ in all cases (Gelman et al., Ch. 11, 2013).

Select contrasts between stations, seasons, experimental period, and temperatures were tested using the function "hypothesis" to examine support for select post-hoc contrasts. A sample hypothesis that would prove an evidence ratio might be, "Anoxic P flux is greater than oxic P flux". To test this hypothesis, we chose to use evidence ratios (ERs), or the ratio of the number of posterior samples consistent with the hypothesis to the number of posterior samples that are

Author Manuscript

inconsistent with the hypothesis, to assess strength of support for each contrast. While we did not assign an arbitrary cutoff value to these ERs, we interpret contrasts with low ER (<5) as having low or no support (Gelman et al., Ch. 5, 2013). We compared fluxes among different models by tabulating the differences between posterior draws and calculating mean differences and ERs as described previously. One core replicate from spring CB2 at 14°C was lost due to incubation system failure, so data from this core are not presented. Several cores incubated at 8°C (including all cores from spring CB4) never reached anoxia due to the temperature limitations on oxygen consumption and higher initial DO solubility, so although samples were analyzed, no fluxes or lag times were calculated.

Results and discussion

During the first portion of the experiment, SRP concentration was uniformly low until anoxia onset, when it began increasing due to flux from the sediment (Fig. 3). During the re-aeration experiment, SRP concentration dropped when the overlying water was removed and replaced with oxygenated (and low-P) water. After the water exchange, SRP concentrations continued to decrease until DO was completely depleted and anoxic P flux from the sediment resumed.

Figure 3: Dissolved oxygen and soluble reactive phosphorus (SRP) concentration over time for spring 2019 core M from site CB2. The blue vertical line represents the onset of anoxic P release during the first portion of the experiment and the black vertical line denotes the beginning of the re-aeration experiment. Labeled flux regions denote time periods where the shown SRP concentrations will be used to calculate fluxes.

Onset of anoxic P flux

Author Manuscript

Table 2 shows that spring and summer sampled cores incubated at 14°C had longer mean lag times (8.66 and 8.90 hours respectively) than fall cores, which displayed a negative mean lag time of -1.26 hours across all sites (i.e., accelerated flux began before anoxia). Lag timing in Table 2 refers to the time between anoxia onset and the time of anoxic P flux onset.

These results show clearly that the accelerated P flux we observed is a symptom of anoxia and not hypoxia, with the notable exception of anoxic P flux occurring hours prior to anoxia in fall. This trend in fall suggests that once sediments have experienced low-DO conditions in situ, as was true for the fall-sampled sediments (Table 1), accelerated soluble P release can occur prior to or upon anoxia onset. This response difference is likely due to a build-up of reduced substances and P in porewater just below the sediment-water interface such that diffusion within the sediment had stronger influence in advance of redox driven release. These reduced substances build up when there is no dissolved oxygen, a normally abundant electron acceptor, to respire them. Metal oxide reduction (including Fe) has been shown to begin prior to anoxia, mobilizing bound P across the sediment-water interface multiple times before full release into overlying water (Hupfer and Lewandowski, 2008; Foster and Fulweiler, 2019).

Author Manuscript

Table 2: Mean estimates of timing (hours with standard error), representing the difference between anoxia onset and anoxic P flux onset for 2019 sediment cores by temperature, season, and central basin (CB) sampling site.

		Hours Between Anoxia and Anoxic P Flux Onset	
		Cores Incubated at 14°C	**Cores Incubated at 8°C**
Spring	**All**	8.66±11.9	20.4±12.5
	CB2	18.0±17.3	17.5±11.3
	CB4	5.57±9.60	NA
	CB5	7.18±11.3	20.2±12.1
Summer	**All**	8.90±11.1	28.0±13.7
	CB2	5.49±9.54	23.5±12.1
	CB4	-1.01±10.4	33.9±19.8
	CB5	27.4±15.5	30.6±17.5
Fall	**All**	-1.26±11.5	23.6±10.2
	CB2	-2.59±10.3	27.1±12.3
	CB4	-3.39±9.34	22.8±8.96
	CB5	-6.48±10.7	19.8±9.36

Oxic and anoxic P flux

Table 3 shows that oxic P flux was lower than anoxic P rates across all seasons, stations, and temperatures. Rates within each phase of the experiment were similar across stations, seasons, and temperatures with some evidence of trends within these categories.

In 14°C cores, anoxic P flux prior to re-aeration ranged from 5.19 – 30.7 mg m^{-2} day^{-1} with an overall mean of 12.8 mg m^{-2} day^{-1} across all seasons and stations. Oxic P flux for 14°C incubated cores ranged from 0.31 – 0.50 mg m^{-2} day^{-1} with an overall mean of 0.38 mg m^{-2} day^{-1}.

Author Manuscript

There was no evidence for differences in oxic P flux between seasons when considered across or within stations. 14°C anoxic P flux was also similar across seasons. However, there was evidence that fall rates were lower than other seasons within stations. This may be due to a higher SRP concentration in the hypolimnion (28.1-36.6 μg L^{-1} in fall versus 2.92-4.54 μg L^{-1} in summer), which could decrease the concentration gradient at the sediment surface and decrease P flux as a result. These hypolimnion sample concentrations were taken at the time of coring and were 6-38x higher during fall across all sites than during spring and summer. Additionally, fall cores had previously experienced low-DO conditions, meaning a portion of the sediment metal oxides may have already been respired and released bound P. This previous P release would mean that fall sediments had a smaller source of bound P relative to other seasons, depressing P flux levels.

As expected, mean anoxic P flux was higher than mean oxic P flux in cores across both temperatures by a factor of 34-55 times. This finding matches the previous results of Matisoff et al. (2016) whose sediment cores from the Western Basin of Lake Erie showed that anoxic P flux was 4-13 times higher than oxic P flux. In terms of previous central basin estimates, anoxic flux reported here are within the range of anoxic P flux (12.8-73.5 mg m^{-2} day^{-1}) from Matisoff et al.'s 1977 sediment core incubations, but higher than those reported by Nürnberg et al., 2019 (7.6 – 8.0 mg m^{-2} day^{-1}). These differences are likely due to the methodology of the different approaches (i.e., core incubations versus estimating flux from changes in in situ SRP concentration). In our parallel in situ mooring study, average anoxic P flux before re-aeration was 11.42 ± 2.6 mg m^{-2} day^{-1} (Anderson et al., 2021). Our mean estimates are generally higher than previous estimates from the central basin, but our range of release rates is inclusive of sediment coring experiment estimates from other lakes such as Matisoff et al.'s 2016 western

Author Manuscript

basin rates of 6.56 ± 6.05 mg m^{-2} day^{-1}, James (2012) who reported anoxic P flux of 8.3-12.5 mg m^{-2} day^{-1} for Lake of the Woods, Minnesota, and Debroux et al. (2012) who estimated anoxic P flux of 6-8 mg m^{-2} day^{-1} from Lake Bard, California. Additionally, Lake Erie central basin P release rates are representative of other eutrophic lakes, (Phillips et al., 2020; Nürnberg, 1997).

Our findings signal that there is a period of time after hypoxia and before anoxia when phosphorus flux is occurring at rates several times slower than anoxic P release rates, and also a lag between anoxic onset and anoxic P flux onset. This timing can be affected if there is a sediment history of anoxic exposure, where previous exposure shortens the time before anoxic P flux onset. Results from this study show that regardless of whether sediments have previously experienced anoxia or are under unfavorable temperature conditions for DO consumption, magnitude of anoxic P flux is similar once accelerated flux begins. Finally, this study measured DO conditions of overlying water rather than of sediment pore water or sediment redox potential. While this approach does not reflect conditions in the sediment, it does relate the flux and onset to dissolved oxygen in the overlying water, which is more readily monitored and makes the results relatable to both modeled and measured patterns of oxygen in the basin. Therefore, we are reporting on the necessity of anoxic conditions in the overlying water to produce this accelerated flux.

Re-aeration experiment anoxic flux

Table 3 shows that re-aerated anoxic flux was similar across stations and seasons with some trends within stations. For re-aerated 14°C cores, anoxic P flux after re-aeration ranged from 5.08 – 61.0 mg m^{-2} day^{-1}, with a mean of 14.8 mg m^{-2} day^{-1}. We found no evidence that re-aerated anoxic P flux differed between seasons across all stations, however there was strong evidence that summer CB4 rates were higher than fall or spring (ER = 166 and 168,

Author Manuscript

424 respectively). When comparing between anoxic P flux and re-aerated anoxic P flux at 14°C,
425 there was no difference at the level of season. The only strong evidence found was that re-
426 aerated anoxic P flux was higher than initial anoxic P flux at CB4 in both spring and summer
427 (ER = 7.21; 799) (see Fig. 4). Anoxic P flux did not change pre- and post-re-aeration, suggesting
428 that re-aerated anoxic P flux behaves similarly in magnitude to the initial anoxic P release rates
429 despite observed faster consumption of DO following re-aeration (seen in Figure 2). It is likely
430 that a build-up of reduced substances at the sediment-water interface and in the overlying water
431 following anoxia contributed to accelerated DO consumption.

432 There are previously reported rates and trends published for re-aerated sediment P
433 release. Zorn et al. (2018) reports average release rates of 20.74 ± 23.3 mg m^{-2} day^{-1} following 8
434 re-aeration events observed in Green Bay using in situ instrumentation. There was no distinct
435 trend in the 8 reported release rates relative to each other, attributed to different sets of properties
436 driving water replacement and P release. Anderson et al. (2021) deployed in situ DO and SRP
437 sensors at the CB2 and CB4 stations used in the present study and found that rates before re-
438 aeration (11.42 ± 2.6 mg m^{-2} day^{-1}) were lower than re-aerated rates (89.1 ± 8.6 mg m^{-2} day^{-1}).
439 There are several potential reasons why the re-aerated rates in the present study were not as high
440 as those observed in Anderson et al. (2021). This in situ study was subject to advection of water
441 during anoxia, which may have increased SRP concentration faster than from sediment flux
442 alone. Also, the sediment core incubation had a lower ratio of overlying water to sediment,
443 which could result in faster buildup of SRP in the water, thereby lowering the release rate from
444 sediment.

445 Temperature effects

Author Manuscript

Comparisons between incubation temperatures showed compelling results in flux onset timing and oxic P flux magnitudes. The overall mean time difference from anoxia to anoxic P flux onset for cores incubated at 8°C was 23.4 hours, and 5.4 hours for cores incubated at 14°C. Comparing between the incubation temperature models, time before anoxic P flux onset was evidently longer across all stations at 8ºC than at 14ºC in summer (ER = 7.46) and fall (ER = 21.6), and similar in spring (ER = 3.50). Among the cores incubated at 14ºC, fall cores tended to have shorter onset than spring or summer, but evidence for this difference was weak. The model for cores incubated at 8°C showed that there was no evidence that onset timing was different across seasons or stations. The onset of anoxic P flux was likely delayed at 8ºC relative to 14°C due to temperature constraints on metabolic oxygen demand which elongated the period of time needed for cores to experience anoxia and for the onset of anoxic P flux to occur. We attribute this delay to temperature dependence of microbial anaerobic respiration that solubilizes iron oxide minerals. Notably, some cores (including all spring CB4 cores) incubated at 8°C never reached anoxia.

Oxic P release rates were higher at 14°C than 8°C during fall (mean difference = 0.51 mg m^{-2} day^{-1}, ER = 26.8) and summer (mean difference = 0.25 mg m^{-2} day^{-1}, ER = 5.18), but similar between the two temperatures in spring (ER = 3.35). Oxic P flux increased as the seasons progressed at 14°C with higher oxic P flux in the fall, but this trend did not occur at 8°C. This trend supports the previous findings that sediments with a history of low-DO exposure experience accelerated P flux sooner. Alternatively, the 8°C cores spent almost a week under oxygenated conditions. This may have been sufficient to 'reset' the changes associated with anoxia that made the 14°C cores more susceptible to anoxic P flux onset.

Author Manuscript

Anoxic P flux was not consistently higher at 14ºC than at 8ºC and did not show substantive differences at the level of season or station, but temperature did affect the length of time required for cores to reach anoxia, as onset of anoxic P flux was delayed at 8ºC compared to 14ºC. These temperatures were chosen in order to represent the range of in situ temperatures measured across the seasons (Table 1), but not every temperature and season combination represents realistic in situ conditions. Specifically, the benthos are likely to be closer to 8ºC in spring and closer to 14ºC in fall. The overall estimate for anoxic flux at these times were similar: 11.5±4.3 mg m^{-2} day^{-1} in spring at 8ºC and 11.9±2.2 mg m^{-2} day^{-1} in fall at 14ºC.

Our temperature range caused results to differ from results in previous studies such as Gibbons and Bridgeman (2020) who noted that anoxic P flux was 2-14 times higher at high incubation temperatures (20-30ºC) representing future climate scenarios compared with cores incubated at 10ºC. Our study examined a smaller range of temperatures, 8ºC and 14ºC, and while a larger range of temperatures would be helpful to produce large effects and understand controls on this process, the hypolimnion of the central basin is likely to become anoxic only when temperatures are warm enough to deplete oxygen but cold enough to remain stratified and prevent mixing. Temperature certainly plays a large role in determining the duration of anoxic conditions in the hypolimnion. Specifically, the strong temperature dependence of oxygen consumption means that anoxia will begin earlier and last longer at warmer temperatures.

Author Manuscript

Table 3: Oxic and anoxic P flux and standard errors for cores incubated at 14°C and 8°C and re-aerated anoxic P flux and standard errors are displayed. The different columns correspond to the portions of the experiment denoted in Figure 3. Each release rate represents the mean flux of all cores grouped by season and site that reached anoxia. Seasonal flux means are reported across stations.

P Flux (mg m^{-2} day^{-1}) for Cores Incubated at 14°C and 8°C						
		14°C Core Incubations			**8°C Core Incubations**	
		Oxic Flux	**Anoxic Flux**	**Re-aerated Anoxic Flux**	**Oxic Flux**	**Anoxic Flux**
Spring	**All**	0.39±0.22	13.1±2.25	13.2±6.33	0.21±0.13	11.5±4.32
	CB2	0.37±0.22	10.8±3.49	9.35±5.38	0.35±0.11	9.65±4.67
	CB4	0.41±0.22	17.1±3.38	10.1±5.21	NA	NA
	CB5	0.39±0.22	11.7±2.77	11.4±4.99	0.14±0.09	9.20±4.70
Summer	**All**	0.34±0.23	13.8±2.30	20.2±7.57	0.09±0.13	13.2±4.27
	CB2	0.33±0.24	15.6±2.65	15.9±6.13	0.08±0.12	15.3±5.33
	CB4	0.36±0.25	14.2±2.33	47.0±8.15	0.13±0.13	12.2±6.62
	CB5	0.32±0.23	13.8±2.77	18.2±5.92	0.08±0.14	11.8±5.73
Fall	**All**	0.45±0.25	11.9±2.22	13.1±6.28	-0.06±0.14	15.1±4.06
	CB2	0.44±0.25	11.2±2.40	8.98±5.13	-0.13±0.14	14.8±4.95
	CB4	0.44±0.25	12.3±2.35	12.8±4.92	-0.01±0.13	21.7±7.25
	CB5	0.48±0.25	9.73±2.65	10.6±5.10	-0.11±0.11	14.2±4.02

Figure 4 shows anoxic P flux and standard errors for 14°C incubated cores grouped by site, season, and before and after re-aeration.

Author Manuscript

Figure 4: Anoxic P flux and standard errors for 14°C incubated sediment cores from sites central basin (CB) sites CB2, CB4, and CB5 are shown for the initial and re-aerated portions of this experiment. Core replicates are represented by the smaller, lighter points while flux means are displayed by the larger and darker points.

Methodological limitations and comparisons

The findings from this study may represent an underestimation of sediment P flux as some released P may have been in the form of dissolved organic P (DOP), which we did not measure but can be an important source of P in some systems (Kurek et al., 2021), or was quickly bound or taken up by particles or biomass. We used SRP as the response variable since it captures the principal component forms that are released from sediments under hypoxia. SRP represents multiple component forms of P that are released from sediments under hypoxia, and past studies such as Nürnberg (1988) and Eckert et al. (2020) have found that the ratio of SRP to TP in the hypolimnion after P release approaches 1:1.

Sediment P flux has been measured in lakes across the spectrum of eutrophic and oligotrophic conditions. Nürnberg (1988)'s review of this literature shows that rates determined across system and methodological variance are constrained by a certain bound (range = 0.25 – 51.5 mg m^{-2} day^{-1}, median rate = 10.24 mg m^{-2} day^{-1}). Our findings are in line with the bounds of this worldwide data. Our findings on anoxic P flux and timing from anoxia to anoxic P flux onset are consistent with a companion study that used in situ remote sensing to observe SRP concentration and flux at the hypolimnion of CB2 and CB4 during summer and fall 2019 (Anderson et al., 2021). This remote sensing study produced lag times of 12 - 42 hours and the ensuing anoxic P flux averages ranged from 11.42 - 25.67 mg m^{-2} day^{-1}. This in situ experiment supports the accuracy of this study's short-term sediment coring incubation methodology, which

Author Manuscript

was employed with a focus on high precision through sampling frequency and core replicates across seasons and locations in order to address a gap in our understanding of the environmental conditions, timing, and rates of internal P flux for the central basin.

The scope of this study is limited to the 2019 coring season, and although it shows variation between seasons, it does not account for interannual environmental variability such as anoxic duration or nitrate concentration in the hypolimnion. Hypoxic and anoxic durations are highly affected by environmental factors such as dissolved oxygen consumption rates, temperature, and biomass production. Another factor that may impact interannual variability in anoxia and P loading is the role of nitrate and other alternative electron acceptors that could impact the rate of depletion of dissolved oxygen. Nitrate in the hypolimnion can control P release from sediments as seen in Eckert et al. (2020) who showed that in consecutive years in Lake Kinneret, Israel elevated levels of hypolimnion nitrate delayed and depressed overall P loading relative to the following year with lower hypolimnion nitrate. Additionally, we found no correlations between fluxes and sediment TP (see Supplemental Information), although it remains possible that the mineralogical or chemical conditions led to different amounts of mobile P that our methods did not characterize.

Importance of timing and flux for seasonal loading

Our findings on the timing and rates of sediment P release are relevant when considering the magnitude and effects of basin-wide P loading that occurs seasonally. Yearly variation in the duration of hypoxia and anoxia affects the length and magnitude of basin-wide loading. The rate and timing estimates from our study are based on a single year of observations, but past years of mooring observations can be used to further contextualize the annual durations of these conditions. Hypoxic durations in 2019 were 67 and 43 days at CB2 and CB4 respectively and

Author Manuscript

were 37 and 50 days in 2018 and 17 and 55 days in 2017. Anoxic durations during the 2019 season were 44 and 27 days at CB2 and CB4 respectively, 7 and 23 days during 2018, and 8 and 37 days during 2017 (NOAA NCEI 0210815 and 0210823). 2019 had more hypoxic and anoxic days than the two preceding years, and there is annual variation in the duration of these low DO conditions. In terms of P release rates, this study produced means and ranges of both anoxic and oxic rates. This study found an overall 14°C anoxic P release rate of 12.8 mg m^{-2} day^{-1} across all seasons and stations with a range of 5.19 – 30.7 mg m^{-2} day^{-1}. The 14°C oxic P flux ranged from 0.31 – 0.50 mg m^{-2} day^{-1} with an average of 0.38 mg m^{-2} day^{-1}. The uncertainties in these parameters affect estimates of total basin-wide loading, which has not been calculated here as the spatial extent and duration of anoxia are poorly constrained by existing observations. For example, hypoxia and anoxia begin at the shallow edges of the hypolimnion (Rowe et al., 2019) so the area of sediment responsible for anoxic P flux at any given point in the season will be smaller than the maximum area overlaid by anoxic water at some point during the season. Nonetheless, approximations of total central basin P loading calculations based on release rates are possible (Anderson et al., 2021).

Our findings on delayed onset of anoxic P flux indicate that sediments will not begin accelerated flux until after anoxia has been established. These findings could have a large effect on total basin internal loading estimates within or across years.

Implications for Lake Erie management and monitoring

Internal loading of phosphorus has been cited as a major challenge for long-term P removal and management in water systems (Giles et al., 2015), and monitoring the extent and impact of internal loading will be particularly important as climate change lengthens the duration of stratification (Mason et al. 2016). These conditions will lead to increasingly longer periods of

Author Manuscript

hypolimnion anoxia and higher average P flux (Gibbons and Bridgeman, 2020), both factors that will increase total internal P loads. These future trends make it vital to constrain internal P loading as a function of DO condition and temperature. Expanded and focused monitoring efforts on anoxia and P would help watershed managers and monitoring programs improve our estimates of internal loading and track how it responds to reductions in loading from the watershed.

Internal loading does not add new P to lakes, but rather recycles legacy sediment P from past external loads, which can contribute to and extend hypoxia and anoxia and impact primary production. This stored internal load has the potential to amplify the effects of current external loads depending on the timing, spatial extent, and duration of conditions that favor accelerated release of internal P and vary annually. However, direct observations linking internal loading to enhanced oxygen demand and hypoxia are not available. Sampling campaigns in the central basin typically conclude around the same time as fall turnover, so the fate of the released SRP is uncertain. Winter studies have shown the increasing significance of winter-spring diatom blooms in the central basin, and high carbon flux seen to winter sediments complements this trend, implying that released SRP may have a part in fueling these blooms (Reavie et al., 2016; Wilhelm et al., 2014). Further work in biophysical modeling, specifically a better understanding of spatial hypoxia and anoxia on an annual basis, will be required to constrain interannual differences and predict bioavailable P fate during and after stratification. As the U.S. and Canada pursue further reductions in external loads, it will be important to monitor the extent of anoxia and also monitor the impact on P distribution during and after stratification.

Literature cited

Author Manuscript

586 Anderson, H.S., Johengen, T.H., Godwin, C.M., Purcell, H., Alsip, P., Ruberg, S., Mason, L.
587 2021. Continuous *in situ* nutrient analyzers pinpoint the onset and rate of internal P
588 loading under anoxia in Lake Erie's Central Basin. Environ. Sci. Technol. Water. doi:
589 10.1021/acsestwater.0c00138.
590
591 Arega, F., Lee, J.H.W. 2005. Diffusional Mass Transfer at Sediment-Water Interface of
592 Cylindrical Sediment Oxygen Demand Chamber. J. Environ. Eng., 131(5): 755-766. doi:
593 10.1061/(ASCE)0733-9372(2005)131:5(755).
594
595 Beletsky, D., Hawley, N., Rao, Y.R. 2013.Modeling summer circulation and thermal structure of
596 Lake Erie. J. Geophys. Res.: Oceans, 118: 6238-6252. doi: 10.1002/2013JC008854.
597
598 Boström, B., Andersen, J.M., Fleischer, S., Jansson, M. 1998. Exchange of phosphorus across
599 the sediment-water interface. Hydrobiol., 170: 229-244.
600
601 Bürkner, P. 2018. "Advanced Bayesian Multilevel Modeling with the R Package brms." The R
602 Journal, 10(1): 395–411. doi: 10.32614/RJ-2018-017.
603
604 Burns, N.M. and Ross, C. 1972. Project Hypo. CCIW Pap 6 US EPA, Tech Rep TS-05071-208-
605 24.
606
607 Caraco, N. 2009. Phosphorus. Reference Module in Earth Systems and Environmental Sciences:
608 Encyclopedia of Inland Waters, 73-78. doi: 10.1016/B978-012370626-3.00097-1.

Author Manuscript

Debroux, J-F., Ceutel, M., Thompson, C., Mulligan, S. 2012. Design and testing of a novel hypolimnetic oxygenation system to improve water quality in Lake Bard, California. Lake and Reservoir Manage., 28: 245-254.

DePinto, J., Young, T., Martin, S. 1981. Algal-Available Phosphorus in Suspended Sediments from Lower Great Lakes Tributaries. J. Great Lakes Res., 7(3): 311-325.

Eckert, W., Beeri-Shlevin, Y., Nishri, A. 2020. Chapter 20: Internal Phosphorus Loading in Sub-tropical Lake Kinneret, Israel, Under Extreme Water Level Fluctuation, p. 377-406. In A.D. Steinman and B.M. Spears [1st ed.], Internal Phosphorus Loading in Lakes: Causes, Case Studies, and Management. J. Ross Publishing.

Edwards, W., Conroy, J., Culver, D. 2005. Hypolimnetic Oxygen Depletion Dynamics in the Central Basin of Lake Erie. J. Great Lakes Res., 31(2): 262-271.

Federal Water Pollution Control Act (Clean Water Act, CWA). 1972. U.S. Government Publishing. https://www.gpo.gov/fdsys/pkg/USCODE-2017-title33/html/USCODE-2017-title33-chap26.htm. Accessed: April 12, 2020.

Foster, S.Q., Fulweiler, R.W. 2019. Estuarine Sediments Exhibit Dynamic and Variable Biogeochemical Responses to Hypoxia. J. Geophys. Res.: Biogeosci., 124. doi: 10.1029/2018JG004663.

Author Manuscript

Gelman, A., Carlin, J.B., Stern, H.S., Rubin, D.B. 2013. Chapter 5: Hierarchical models; Chapter 11: Basics of Markov Chain Simulation. Bayesian Data Analysis. CRC Press LLC.

Gerling, A., Munger, Z., Doubek, J., Hamre, K., Gantzer, P., Little, J., Carey, C. 2016. Whole-Catchment Manipulations of Internal and External Loading Reveal the Sensitivity of a Century-Old Reservoir to Hypoxia. Ecosyst., 19: 555-571.

Giles, C., Isles, P., Manley, T., Xu, Y., Druschel, G., Schroth, A. 2015. The mobility of phosphorus, iron, and manganese through the sediment-water continuum of a shallow eutrophic freshwater lake under stratified and mixed water-column conditions. Biogeochemistry, 127: 15-34.

Gibbons, K.J., Bridgeman, T.B. 2020. Effect of temperature on phosphorus flux from anoxic western Lake Erie sediments, Water Res., doi: 10/1016/j.watres.2020.116022.

Hupfer, M., Lewandowski, J. 2008. Oxygen Controls the Phosphorus Release from Lake Sediments – a Long-Lasting Paradigm in Limnology. Int. Rev. Hydrobiol., 93(4-5): 415-432. doi: 10.1002/iroh.200711054.

Ivey, G.N., Boyce, F.M. 1982. Entrainment by Bottom Currents in Lake Erie. Limnol. Oceanogr., 27(6): 1029-1038.

Author Manuscript

James, W.F. 2012. Estimation of Internal Phosphorus Loading Contributions to the Lake of the Woods, Minnesota. ERDC Report, 42 pp.

Kurek, M.R., Harir, M., Shukle, J.T., Schroth, A.W., Schmitt-Kopplin, P., Druschel, G.K. 2021. Seasonal transformations of dissolved organic matter and organic phosphorus in a polymictic basin: Implications for redox-driven eutrophication. Chem. Geol., 573: 120212.

Lee, J.H.W., Kuang, C.P., Yung, K.S. 2000. Analysis of three-dimensional flow in a cylindrical sediment oxygen demand chamber. Appl. Math. Model., 24: 263-278.

Mason, L., Riseng, C., Gronewold, A., Rutherford, E., Wang, J., Clites, A, Smith, S., McIntyre, P. 2016. Fine-scale spatial variation in ice cover and surface temperature trends across the surface of the Laurentian Great Lakes. Climatic Change, 138: 71-83.

Matisoff, G., Fisher, J.B., Lick, W. 1977. Early Diagenesis and Chemical Mass Transfer in Lake Erie Sediments. US EPA Large Lakes Research Station, Contract No. R805716020.

Matisoff, G., Kaltenberg, E., Steely, R., Hummel, S., Seo, J., Gibbons, K., Bridgeman T., Seo, Y., Behbahani, M., James, W., Johnson, L., Doan, P., Dittrich, M., Evans, M.A., Chaffin, J. 2016. Internal loading of phosphorus in western Lake Erie. J. Great Lakes Res., 42: 775-788.

Author Manuscript

Mohamed, M., Wellen, C., Parsons, C.T., Taylor, W., Arhonditsis, G., Chomicki, K., Boyd, D., Weidman, P., Mundle, S., Van Cappellen, P., Sharpley, A., Haffner, G. 2019. Understanding and managing the re-eutrophication of Lake Erie: Knowledge gaps and research priorities. Freshwater Sci., 38(4): 675-691. doi: 10.1086/705915.

Mortimer, C. 1971. Chemical Exchanges Between Sediments and Water in the Great Lakes-Speculations on Probably Regulatory Mechanisms. Limnol. Oceanogr., 16(2). doi: 10.4319/lo.1971.16.2.0387.

National Oceanic and Atmospheric Administration, Great Lakes Environmental Research Laboratory; Cooperative Institute for Great Lakes Research, University of Michigan. 2020. Water physical, chemical, and biological vertical observational data at multiple levels from fixed mooring CHRP2 and CTD casts taken from NOAA research vessel R5501 in the central basin of Lake Erie, Great Lakes region from 2017-06-09 to 2019-10-10 collected by National Oceanic and Atmospheric Administration, Great Lakes Environmental Research Laboratory and the Cooperative Institute for Great Lakes Research, University of Michigan. (NCEI Accession 0210815). NOAA National Centers for Environmental Information. Dataset. https://accession.nodc.noaa.gov/0210815. Accessed 09/28/2020.

National Oceanic and Atmospheric Administration, Great Lakes Environmental Research Laboratory; Cooperative Institute for Great Lakes Research, University of Michigan. 2020. Water current profile, physical, and chemical vertical observational data at multiple

Author Manuscript

levels from fixed mooring CHRP4 and CTD casts taken from NOAA research vessel R5501 in the central basin of Lake Erie, Great Lakes region from 2017-05-23 to 2019-10-10 collected by National Oceanic and Atmospheric Administration, Great Lakes Environmental Research Laboratory and the Cooperative Institute for Great Lakes Research, University of Michigan. (NCEI Accession 0210823). NOAA National Centers for Environmental Information. Dataset. https://accession.nodc.noaa.gov/0210823. Accessed 09/28/2020.

National Oceanic and Atmospheric Administration, Great Lakes Environmental Research Laboratory; Cooperative Institute for Great Lakes Research, University of Michigan. 2020. Water current profile, physical, and chemical vertical observational data at multiple levels from fixed mooring CHRP5 and CTD casts taken from NOAA research vessel R5501 in the central basin of Lake Erie, Great Lakes region from 2017-05-23 to 2019-10-08 collected by National Oceanic and Atmospheric Administration, Great Lakes Environmental Research Laboratory and the Cooperative Institute for Great Lakes Research, University of Michigan (NCEI Accession 0210822). NOAA National Centers for Environmental Information. Dataset. https://accession.nodc.noaa.gov/0210822. Accessed 09/28/2020.

Nürnberg, G. 1984. The prediction of internal phosphorus load in lakes with anoxic hypolimnia. Limnol. Oceanogr., 29(1): 111-124.

Author Manuscript

723 Nürnberg, G. 1988. Prediction of phosphorus release rates from total and reductant-soluble
724 phosphorus in anoxic lake sediments. Can. J. Fish. Aquat. Sci., 45: 453-462.
725
726 Nürnberg, G. 1991. Phosphorus from internal sources in the Laurentian Great Lakes, and the
727 concept of threshold external load. J. Great Lakes Res., 17(1): 132-140.
728
729 Nürnberg, G. 1997. Coping with water quality problems due to hypolimnetic anoxia in Central
730 Ontario Lakes. Water Qual. Res. J. Can., 32: 391-405.
731
732 Nürnberg, G., Howell, T., Palmer, M. 2019. Long-term impact of Central Basin hypoxia and
733 internal phosphorus loading on north shore water quality in Lake Erie. Inland Waters,
734 9(3): 1-12. doi: 10.1080/20442041.2019.1568072.
735
736 Paytan, A., Roberts, K., Watson, S., Peek, S., Chuang, P-C., Defforey, D., Kendall, C. 2017.
737 Internal loading of phosphate in Lake Erie Central Basin. Sci. Total Environ., 579: 1356-
738 1365.
739
740 Phillips, G., Kelly, A., Pitt, J-A., Spears, B.M. 2020. Chapter 13: Barton Broad, UK: Over 40
741 Years of Phosphorus Dynamics in a Shallow Lake Subject to Catchment Load Reduction
742 and Sediment Removal, p. 243-262. In A.D. Steinman and B.M. Spears [1st ed.], Internal
743 Phosphorus Loading in Lakes: Causes, Case Studies, and Management. J. Ross
744 Publishing.
745

Author Manuscript

Reavie, E., Cai, M., Twiss, M., Carrick, H., Davis, T., Johengen, T., Gossiaux, D., Smith, D., Palladino, D., Burtner, A., Sgro, G. 2016. Winter-spring diatom production in Lake Erie is an important driver of summer hypoxia. J. Great Lakes Res., 42(3): 608-618.

Rowe, M., Anderson, E., Beletsky, D., Stow, C., Moegling, S., Chaffin, J., May, J., Collingsworth, P., Jabbari, A., Ackerman, J. 2019. Coastal Upwelling Influences Hypoxia Spatial Patterns and Nearshore Dynamics in Lake Erie. J. Geophys. Res.: Oceans, 124(8): 6154-6175. doi: 10.1029/2019JC015192.

Rowland, F., Stow, C., Johengen, T., Burtner, A., Palladino, D., Gossiaux, D., Davis, W., Johnson, L., Ruberg, S. 2020. Recent Patterns in Lake Erie Phosphorus and Chlorophyll *a* Concentrations in Response to Changing Loads. Environ. Sci. Technol., 54: 835-841.

Ruberg, S., Guasp, E., Hawley, N., Muzzi, R., Brandt, S., Vanderploeg, H., Lane, J., Miller, T. 2008. Societal Benefits of the Real-Time Coastal Observation Network (ReCON): Implications for Municipal Drinking Water Quality. Mar. Technol. Soc. J., 42(3): 103-109.

Scavia, D., David Allan, J., Arend, K. K., Bartell, S., Beletsky, D., Bosch, N. S., Brandt, S.B., Briland, R., Daloğlu, I., DePinto, J., Dolan, D., Evans, M.A., Farmer, T., Goto, D., Han, H., Höök, T., Knight, R., Ludsin, S., Mason, D., Michalak, A., Richards, P., Roberts, J., Rucinski, D., Rutherford, E., Schwab, D., Sesterhenn, T., Zhang, H., Zhou, Y. 2014.

Author Manuscript

Assessing and addressing the re-eutrophication of Lake Erie: Central basin hypoxia. J. Great Lakes Res., 40(2): 226-246. doi: 10.1016/j.jglr.2014.02.004.

Scavia, D., Bertani, I., Obenour, D.R., Turner, R.E., Forrest, D.R., Katin, A. 2017a. Ensemble modeling informs hypoxia management in the northern Gulf of Mexico. PNAS, 114: 8823-8828.

Scavia, D., Kalcic, M., Muenich, R. L., Read, J., Aloysius, N., Bertani, I., Boles, C., Confesor, R., DePinto, J., Gildow, M., Martin, J., Redder, T., Robertson, D., Sowa, S., Want, Y., Yen, H. 2017b. Multiple models guide strategies for agricultural nutrient reductions. Front. Ecol. Environ., 15(3): 126-132.

Seal AA3 AutoAnalyzer Manual. Method No. G-297-03 Rev. 5 (Multitest MT 19).

Snodgrass, W., Fay, L. 1987. Values of Sediment Oxygen Demand Measured in the Central Basin of Lake Erie, 1979. J. Great Lakes Res., 13(4): 724-730.

Stan Development Team. 2020. RStan: the R interface to Stan. R package version 2.21.2. http://mc-stan.org/.

Steinman, A.D., Spears, B.M. 2020. Chapter 1: What Is Internal Phosphorus and Why Does It Occur?, p. 3-14. In A.D. Steinman and B.M. Spears [1st ed.], Internal Phosphorus Loading in Lakes: Causes, Case Studies, and Management. J. Ross Publishing.

Author Manuscript

Stone, J.P., Pangle, K.L., Pothoven, S.A., Vanderploeg, H.A., Brandt, S.B., Höök, T.O., Johenged, T.H., Ludsin, S.A. 2020. Hypoxia's impact on pelagic fish populations in Lake Erie: a tale of two planktivores. Can. J. Fish. Aquat. Sci., 18: 1-18. doi: 10.1139/cjfas-2019-0265.

Vahtera, E., Conley, D., Gustafsson, B., Kuosa, H., Pitkänan, H., Savchuk, O., Tamminen, T., Voss, M., Wasmund, N., Wulff, F. 2007. Internal Exosystem Feedbacks Enhance Nitrogen-fixing Cyanobacteria Blooms and Complicate Management in the Baltic Sea. Ambio., 36(2/3): 186-194.

Wilhelm, S. W., G. R. LeCleir, G. S. Bullerjahn, R. M. McKay, M. A. Saxton, M. R. Twiss, and R. A. Bourbonniere. 2014. Seasonal changes in microbial community structure and activity imply winter production is linked to summer hypoxia in a large lake. FEMS Microbiol. Ecol., 87: 475-485.

Zhang, H., Boegman, L., Scavia, D., Culver, D.A. 2016. Spatial distributions of external and internal phosphorus loads in Lake Erie and their impacts on phytoplankton and water quality. J. Great Lakes Res., 42(6): 1212-1227. doi: 10.1016/j.jglr.2016.09.005.

Zhou, Y., Obenour, D., Scavia, D., Johengen, T., Michalak, A. 2013. Spatial and Temporal Trends in Lake Erie Hypoxia, 1987-2007. Environ. Sci. Technol., 47: 899-905.

Author Manuscript

814 Zorn, M., Waples, J., Valenta, T., Kennedy, J., Klump, J.V. 2018. *In situ*, high-resolution time
815 series of dissolved phosphate in Green Bay, Lake Michigan. J. Great Lakes Res., 44: 875-
816 882.

Author Manuscript

Acknowledgements:

This work was supported by the National Oceanic and Atmospheric Administration's National Centers for Coastal Ocean Science Competitive Research Program under award NA16NOS4780209 to the University of Michigan, the Great Lakes Restoration Initiative (GLRI), Cooperative Science and Monitoring Initiative (CSMI), and through the NOAA Cooperative Agreement with the Cooperative Institute for Great Lakes Research (CIGLR) at the University of Michigan (NA17OAR4320152). This is CIGLR contribution no. 1183 and CHRP contribution no. 256. This work was supported by vessel crew Daniel Burlingame, Todd Roteman, and Kent Baker. Ashley Burtner assisted with measuring phosphorus samples. Lacey Mason produced Figure 1. Three reviewers provided comments on this manuscript which greatly improved the quality and clarity of our study.

No conflicts of interest were reported for this study. Data and R code is available upon request to the corresponding author.

Author Manuscript